Calhoun: The NPS Institutional Archive
DSpace Repository

Theses and Dissertations 1. Thesis and Dissertation Collection, all items

1951

Investigation of the air-flow in an acoustic jet at resonance.

Janes, Ralph C.

University of Minnesota

http://hdl.handle.net/10945/14293

Downloaded from NPS Archive: Calhoun

Calhoun is the Naval Postgraduate School's public access digital repository for research materials and institutional publications created by the NPS community. Calhoun is named for Professor of Mathematics Guy K. Calhoun, NPS's first appointed -- and published -- scholarly author.

Dudley Knox Library / Naval Postgraduate School
411 Dyer Road / 1 University Circle
Monterey, California USA 93943

http://www.nps.edu/library

Janes

Investigation of the airflow in an acoustic jet at resonance.

Thesis
J28

Library
U. S. Naval Postgraduate School
Annapolis, Md.

[illegible] OF THE [illegible]
[illegible] AT [illegible]

A Thesis

Submitted in Partial Fulfillment of the Requirements

for the

Master of Science Degree in Aeronautical Engineering

at the University of Minnesota

by

Ralph J. [illegible]

[illegible]

[illegible]

A Thesis
Submitted in Partial Fulfillment of the Requirements
for the
Master of Science Degree in Agricultural Engineering
in the University of Illinois

by

Ralph C. [illegible]

[illegible]

Thesis
C41

TABLE OF CONTENTS

Summary 1

Introduction 3

Nomenclature 5

Related Theory 8

Description of Apparatus and Procedure 13

Results and Discussion 32

Conclusions 15

Bibliography 16

16259

LIST OF FIGURES

Figure 1. Principle Apparatus

Figure 2. Mechanical Oscillator

Figure 3. Resonator Open End Modification with "Wall Static" Instrumentation

Figure 4. External Traverse Arrangement

Figure 5. Internal Traverse Arrangement

Figure 6. Resonator Mean Static and Total Pressure Distribution in Axial Direction

Figure 7. Mean Pressure Distribution in Plane along Resonator Axis of Symmetry

Figure 8. Resonator Wall Static Pressure Distribution for Various Magnitudes of Piston Stroke

Figure 9. Resonator Wall Mean Static Pressure versus Piston Stroke, with Distance from Resonator Open End as a Parameter

Figure 10. Effect of Open End Shape on Mean Static Pressure at the Resonator Surface

Figure 11. Effect of Frequency on Mean Static Pressure at the Resonator Surface for Fixed Resonator Length

Figure 12. Effect of Frequency on Mean Static Pressure at the Resonator Wall for Selected Stations

Figure 13. Determination of Resonant Frequency for Basic Resonator Configuration by Measuring the Mean Static Pressure at the Resonator Surface

Figure 14. Determination of Resonant [illegible] for Tapered Tip Resonator Configuration

Figure 15. [illegible] for Basic Resonator Configuration

Figure 16. Internal Radial Profile, Mean Static Pressure

LIST OF FIGURES (cont.)

Figure 17. Mean Pressure Profile [illegible] Outside of Resonator Open End

Figure 18. Internal Radial Traverse Mean Total Pressure

Figure 19. Dust Figures and Jet at Low Piston Stroke

Figure 20. Dust Ridges Near Open End after Run at a Piston Stroke of 0.302 in.

Figure 21. Dust Figure Leading into Jet at a Piston Stroke of 0.954 in.

Figure 22. Dust Figure Leading into Jet with Smoke Showing Edge Vortex at a Piston Stroke of 0.954 in.

Figure 23. Same as Figure 22 except that Downstream Detail of Jet is More Sharply Outlined

Figure 24. Close-up of Dust Figure; not visible is the observed fact that these tiny particles are describing straight oscillatory paths parallel to the axis. Dots at the top are six inches apart.

Figure 25. Penetration of Edge Vortex at a Piston Stroke of 0.702 in.

Figure 26. Penetration of Edge Vortex at a Piston Stroke of 0.954 in.

Figure 27. Variation of Depth of Penetration of Resonator, by End Vortex System, with Magnitude of Piston Stroke

Figure 28. Oscillating Particles of Dust Near Resonator Open End (between Stas. 0 and 1) at a Piston Stroke of 0.302 in.

Figure 29. Oscillating Particles of Dust at Same Location as Above but at a Piston Stroke of 0.954 in.

Figure 30. Estimated Dust Particle Path Length for Different Magnitudes of Piston Stroke

Figure 31. Variation of Estimated Dust Particle Path Length with Piston Stroke

Figure 32. Idealized Time-Distance Diagram of Wave Fronts in a Resonator Closed at One End by a Pulsator and Open at the Other End

SUMMARY

The airflow phenomenon, known as an "acoustic jet" and associated with an open-end resonator excited by an oscillator, was investigated using a mechanical, piston-type pulsator with piston stroke variable in the range of zero to one inch. The objective was the quantitative examination of the mean pressure distribution by liquid manometer measurements, and the determination of the overall flow patterns and behavior, using flow-visualization techniques.

The work grew out of two recent investigations relating the acoustic phenomenon to dynamic thrust, one of which was done at the United Aircraft Corporation Research Department (Ref. 1), and the other of which was done at the University of Minnesota by R. A. Striker (Ref. 2).

Lateral and longitudinal mean pressure gradients are presented for a basic configuration showing the general character of the pressure distribution and the effect of variation of amplitude of pulsating vibration.

The air inside the major portion of the resonator appeared to be pulsating longitudinally without mean flow or general circulation. An external circulation was evident which

involved a pulsed inflow through an open-edge orifice, an apparent reversal, and an efflux through a central jet. The penetration of the end vortex system was found to increase with increased amplitude of piston stroke, but was relatively shallow and appeared to consist mainly of air which was part of the external circulation.

The work was carried out in the Engines Laboratory of the Mechanical and Aeronautical Engineering Departments of the University of Minnesota, under the guidance of Dr. N. A. Hall, and as a preliminary phase of a much broader investigation to be performed by the University with United Aircraft Research Department support.

INTRODUCTION

Many phenomena encountered in the jet propulsion field remain obscure and little understood. Among the foremost of the problems requiring further analysis and investigation are those relating to intermittent and pulsating gas flow. Resonance phenomena are utilized to regulate the gas flow in the pulse-jet. The airflow phenomenon known as the "acoustic jet" is associated with various configurations of tubes or resonators, closed at one end, and excited by a pulsator. Interest has been heightened by the long established fact that under certain conditions a significant amount of thrust is produced by these simple devices with only a small input of energy to the pulsator. Further, engineers testing jet engines have sometimes observed performance improvement associated with resonance.

A comprehensive summary of the historical background, basic acoustic theory, and the nature of early investigations in this field, has been given by Streiter /2/ as part of his report relating the acoustic phenomena directly to static thrust. Other recent investigations include that at Cornell Aeronautical Laboratory (CAL) (Refs. 3, 4, 5), United Aircraft (Ref. 1). Although significant mathematical treatments of wave propagation in tubes of this nature are available (Rayleigh /6/, Stewart /7/

LeMart /13/, Wood /9/, Morse /7/, and Refs 5, 6, 7), it appears that further analysis and investigation is needed in the case of the acoustic jet.

Previous investigations (Refs. 1, 2) have concentrated largely on directly relating the acoustic phenomena to thrust and have shown among other things that the acoustic jet thrust is extremely sensitive to open-end edge conditions, and that it is possible to increase the thrust by increasing the amplitude of the forcing vibration. A broad program of further quantitative and qualitative determination of the flow fields in acoustic jets is needed for the attainment of adequate understanding of this special problem and for further insight into the general characteristics of pulsating flow. Pressure surveys, paralleling the thrust investigations, are needed.

A mechanical pulsator was designed and built by the University of Minnesota Mechanical Engineering staff for use in a broad program of research in pulsating phenomena employing both mean and instantaneous observations. This program was made feasible by United Aircraft Research Department support. The pulsator was kindly made available for the present work which was proposed as a preliminary phase of the broad program.

The primary objectives were twofold; (1) verification

of the flow patterns and behavior employing tufts, smoke, and dust as flow vizualization techniques, and thus establishing, if possible, the salient characteristics of the flow associated with the basic resonator configuration in the available range of amplitude of pulsator vibration; (2) obtaining mean static and total pressure data, using liquid manometer measurements, showing mean pressure distribution in the basic resonator and jet excited by the highest available (about one inch) amplitude of pulsator vibration.

The work was carried out in the Engines Laboratory of the Mechanical and Aeronautical Engineering Departments of the University of Minnesota, under the guidance of Dr. N. A. Hall. The author wishes to express his appreciation for the use of the pulsator, which was made possible through United Aircraft Research Department support, and to express his thanks and appreciation to the following: Dr. N. A. Hall, for his direction and counsel; Professor E. L. Murphy, for his suggestions; Ass't. Professor E. L. Kelly, for his suggestions and assistance.

NOMENCLATURE

h_s	Gage mean static pressure, inches of water, referred to atmospheric pressure.
h_o	Gage mean total pressure, inches of water, referred to atmospheric pressure.
H_a	Ambient atmospheric pressure, inches of mercury, absolute.
t	Ambient atmospheric temperature, degrees Fahrenheit. Also used for time in seconds.
T	Absolute temperature, degrees Rankine. Thrust in lbs.
X	Distance along resonator axis, in inches, measured from the plane normal to the axis, at the open end of the resonator, towards the closed end (piston).
$-X$	Same as X except measured in the other direction (external).
x	General variable for distance along resonator measured from plane of closed end.
L	Resonator length in inches.
ϕ	Angular position in degrees in the plane normal to the resonator axis; referred to a zero line extending from the axis vertically upward, and increasing in a clockwise direction as the observer faces the closed resonator end from the open end. This is used in the Tables (see Table VII and subsequent tables through XII) to indicate the position and direction of the probe at the introduction point. Thus, in Table VII, the static wall pressure at the probe introduction point is at the top of the pressure data column for 0° and for 90°, and is at the bottom of the pressure data column for 180° and for 270°.
r	Radial distance from the resonator axis in inches, positive along the line defining ϕ; negative along the line defining $\phi + 180°$.

r^1	Distance, in inches, measured from the inside resonator wall along a line extending through, and normal to, the resonator axis. Thus it has its largest magnitude at the resonator axis. It is not used negatively.
RPM & N	Revolutions per minute of the pulsator crankshaft unless reference is to some other mechanism.
S	Piston stroke in inches measured from head-end dead center.
R	Crank radius in inches.
L	Center to center length of connecting rod in inches.
θ	Angular position of the pulsator crank from head-end dead center.
V	General velocity variable.
u	Velocity paralleling resonator axis, positive in direction of positive x.
a	Speed of propagation of a sound wave.
f	Frequency, cycles per second.
ω	Angular velocity, radians per second.

Terms Used in Tables

Basic Resonator Configuration. Refers to the basic resonator configuration as described in detail under Apparatus.

Wall Static. Refers to the instrumentation arrangement described, and so referred to, in the section on Apparatus.

Internal Traverse. Refers to the instrumentation arrangement described, and so referred to, in the section on Apparatus.

External Traverse. Refers to the instrumentation arrangement described, and so referred to, in the section on Apparatus.

__Square.__ Used with reference to the open end edge of the resonator, it signifies that the tube was cut squarely off in a plane normal to the axis and that the resulting edge was not modified by tapering.

__Sharp.__ Used with reference to the open end edge of the resonator, it signifies that the edge was tapered to a sharp edge coincident with the end of the inner wall.

RELATED THEORY

The elementary theory, concerning the possible resonant modes of vibration in air columns traversed by plane pressure waves or impulses, is well established and appears in most text books on sound (Refs. 7, 8). It should suffice to review briefly the theory directly related to the resonator configuration which was used in this work, namely, a circular tube open at one end and closed at the other.

Single Resonator Theory

Pressure impulses produced in a tube by plane surfaces normal to the axis are generally assumed to propagate as plane pulses or waves. These waves reflect where area discontinuities occur. Upon encountering a plane wall, as a closed end of a tube, they reflect without a change of phase. Upon encountering an "openness", as at the open end of a tube, they reflect with a one-hundred eighty degree change of phase, i.e., compression waves are reflected as expansion waves and expansion waves are reflected as compression waves. These waves travel at local sonic velocity or higher with respect to the air particles and depending upon their strength. When the tube length and frequency of oscillation are related in such a way that reflected waves return

at the origin just as a new pulse of the same phase is starting, reinforcement occurs, the sound gets greatly increased strength, and it is said that the tube is resonating.

The wave length is four times the distance between a node and the adjacent antinode since the antinode represents a point of instantaneous one-hundred eighty degree change of phase. Then there must always be an antinode at the open end of a resonating tube and a node at the closed end. From these considerations it is easy to deduce the resonant wave length, period, and frequency. For the tube closed at one end and open at the other, we follow the progress of a compression through a complete cycle. A compression wave is started at the closed end, reflected at the open end as a rarefaction, reflected again from the closed end as a rarefaction, and finally from the open end as a compression which returns to the origin completing the cycle after traversing four times the tube length. This is the fundamental mode of vibration for this tube configuration. The wave length is therefore 4L, the period is 4L/c, and the frequency is c/4L. The harmonics would occur at higher frequencies of 3c/4L, 5c/4L, etc.

Since the front of a [illegible] [illegible] which [illegible]

experiment that an "end correction" is needed. Thus, the generally accepted formula for the fundamental frequency of such a resonator is (Ref. 1).

$$f = a/4(L + 0.6r) \qquad (1)$$

Idealized Time-Distance Diagram

Carrying along the assumptions inherent in the simple theory given above, and adding the additional assumption that the compressions and rarefactions are weak plane waves produced instantaneously at the mid-stroke positions of the piston, it is of interest to follow the progress of these compressions and rarefactions in an idealized time-distance diagram ("x-t" diagram) such as is shown in Figure 2a. The small arrows indicate the direction of the velocity increments following, and preceded by, the waves. The circled numbers indicate that the strength of the waves is still [illegible]. Physically, [illegible] all loss mechanisms enter into the actual situation is that a point of equilibrium is reached when the energy input of the piston is balanced with the losses, and at that point the waves have reached their maximum strength.

Piston Motion

The motion of the piston is of interest because it originates the pulses and determines the boundary conditions at the closed end. The pulsator employed in this investigation was equipped with a conventional crank-pin and connecting rod linkage with provision for adjusting the piston stroke in the range of zero to one inch. Thus (Ref. 10), the piston displacement from head-end dead center (x) is:

$$x = L + R - (L^2 - R^2 \sin^2 \theta)^{\frac{1}{2}} - R \cos \theta \qquad (2)$$

where L is the center-to-center length of the connecting rod; R is the crank radius; and θ is the angular position of the crank from head-end dead center. The approximate piston velocity (V) in feet per second is:

$$V = 0.008727NR(\sin \theta + \tfrac{\lambda}{2}\sin 2\theta) \qquad (3)$$

where N is RPM; R is in inches; and λ = R/L. The approximate acceleration of the piston velocity (A) in feet per sec.² is:

$$A = 0.000914N^2R(\cos \theta + \lambda \cos 2\theta) \qquad (4)$$

where the units are as before.

Additional Wave Theory

Reinforcement of a cumulative nature is taking place at resonance, so that the final level of pulse strength is difficult to predict. If the coordinates are transferred to the disturbance front, it is evident that the approach velocity of the flow relative to the traveling pulse is never less than sonic and may be somewhat greater depending on what the final level of pulse strength and temperature distribution actually is. It is shown in aerodynamics texts that the local velocity of wave propagation is a function of the local absolute temperature, thus (Ref. 16):

$$a = \sqrt{g \gamma RT} = \sqrt{\gamma P/\rho} \qquad (5)$$

where the units must be consistent.

There are certain fundamental physical differences between compressive waves and expansive waves. Some of these are ordinarily considered negligible when treating weak isolated waves, but are by no means so when dealing with strong waves or the conditions produced by the repetitive passage of a great many weak waves. It may be shown (Ref. 15) that if a finite, continuous, compressive wave be started, such as by a piston moving reciprocally in a tube, each point of this disturbance, though it

of it a small step wave, each propagates itself at the local speed of sound, relative to the fluid at that point, and will therefore overtake the initial increment of the wave, after a finite time, to form a discontinuity such that the compression takes place practically instantaneously. This must occur because the pulse of a compression wave is characterized by an increase in entropy and temperature (and thus velocity of propagation) over the approach conditions. The time required for this to occur is given as (Ref. 15, p. 47).

$$t = (2/\gamma + 1)\,(1/m) \qquad (6)$$

where $m = (du/dx)_{max}$, the maximum slope of the impressed velocity-distance curve. If the maximum slope of the velocity-distance curve for the piston be taken as a crude approximation of that value, one finds, for the case of one-inch piston stroke and 1000 RPM related to a nine foot long resonator, that the time required to form a discontinuity would be approximately 0.050 seconds, while the time required for the pulse to reach the open end of the resonator would be approximately 0.008 seconds so that a discontinuity is not formed. Only if the reinforcement reached the point where the actual slope of the velocity-distance curve for the flow over the piston was six or seven times the value for the piston, [illegible] discontinuities

would appear near the open end of the resonator.

The reverse situation is true for an expansion wave. Each succeeding increment of such a wave finds itself travelling in a slightly cooler medium than the increment which preceded it, and thus at a slightly lower rate. Thus expansion waves tend to become less steep and be spread out. There is no natural mechanism for the formation of a discontinuous expansion wave (Ref. 15). The approach flow velocity relative to an expansion wave receives an increment of velocity increase, whereas compressive waves impart a decrement.

Measurement of Oscillatory Pressures

Special problems arise in connection with the simplest measurements of oscillating pressures. The fluid is alternately flowing in and then out of the measurement transmission system and this is a non-isentropic process involving flow work and accompanying pressure losses. The natural frequency of the instrumentation, if excited, may completely distort the actual picture. The main factors are therefore: attenuation, resonance, and lag.

Attenuation refers to the pressure drop along a tube due to viscous forces (not resonance effects) and is generally calculated on the basis of Poiseuille's law of viscous resistance

which is given as (Ref. 11):

$$\partial p/\partial x = -(128/\pi)(\mu_0/D^4)Q \qquad (13)$$

where p is the instantaneous pressure at any point in the connecting tube; x is the distance along the tube measured from the entrance; μ_0 is the mean fluid viscosity; D is the tube diameter; Q is the volumetric flow at any point in the tube. Equation (13) is combined with the non-steady, one-dimensional form of the equation of continuity, in Ref. 11, to obtain a solution for values of the loss in ratio of amplitude of pressure for instantaneous pressure measurement devices. Sinusoidal variation at the entrance is assumed (about the mean pressure), and it is assumed that the instrumentation has been designed so as to avoid acoustic resonance effects.

An earlier work (Ref. 10) offers a solution which ignores the variation with time, and is perhaps more suited to estimation of the attenuation effect on mean pressure measurements.

In this case, equation (13) was integrated directly, assuming constant volume flow per unit time, to give, for laminar flow ($0 \leq Re \leq 2000$).

$$p_1 - p_2 = (128Q\mu/\pi D^4)L \qquad (14)$$

and for turbulent flow (2000 ≦ N_R ≦ 100,000),

$$P_1 - P_2 = 1/8(4/\pi)^{7/4}\left(\frac{\mu^{1/4}}{\rho_0}\right)\left(\frac{Q^{7/4}}{D^{19/4}}\right)L \qquad (17)$$

where the units used be consistent, Q is the mass rate of flow, and the pressures P are mean values at the entrance and receiving end respectively. A criterion for determining the type of flow was given as a condition for laminar flow, where the critical Reynolds Number was taken as 2000. Thus,

$$D^3 \Delta_p/L < 3.14 \times 10^{-8} \qquad (18)$$

for laminar flow, where D is in inches and Δ_p/L is pressure drop in inches of mercury per foot of tubing.

Response is the ratio of the value of the measurand at the sensing element to the corresponding value at the entrance of the transmission line. Thus, if the attenuation were zero, the response ratio would give just the effect of natural frequency oscillation in the measuring system. This is given particular attention in NACA TN 1419 (Ref. 18). The electrical analogy is made. The cases of systems with and without negligible instrument volume are treated, as well as amplitude characteristics of systems having an inlet restriction. No theoretical method of predicting the attenuation characteristics of the tubing is given.

The lay is the [illegible] tendency [illegible] [illegible] the [illegible] and the [illegible] [illegible]. This is [illegible] [illegible] with [illegible] and [illegible]. 11.

DESCRIPTION OF APPARATUS AND PROCEDURE

The principal apparatus in this investigation consisted of the mechanical pulsator which could be adjusted in piston stroke amplitude, the resonator, flame chamber, manometers, various probes, apparatus for producing sound and introducing smoke and dust, special lighting, and a variable-speed DC dynamometer as a power source.

The power source (see Figure 2) was a variable-speed, direct current, laboratory test type, electric dynamometer which had ratings: rpm, 1700/2500; HP, 75/100; Amps., 285; Volts, 250.

The mechanical pulsator (see Figure 1) was designed and built by the University of Minnesota Mechanical Engineering Shops with the support of the [illegible] Corporation Research Department. A small flywheel was splined to a shaft that was direct coupled to the dynamometer and supported in two bearings. A crank pin projected from a small, circular plate which bolted to the flywheel with two bolts. Taking advantage of the properties of an ellipse, a pattern of holes was made in the flywheel such that it was only necessary to put the two bolts in a different pair of holes to change the crank radius and thus the

piston stroke. [illegible] counterweight holes in the flywheel made eight possible piston stroke magnitudes available in the range of [illegible] to [illegible] inch. The values of piston stroke used in this investigation were, in inches: ([illegible], [illegible], [illegible], [illegible], [illegible]). These values included the minimum and the maximum for the apparatus. A needle pin bearing connecting rod (five in. long, center to center) was connected to a thrust shaft. The thrust shaft was provided with a guide bearing. The piston screwed on to the head end of the thrust shaft and fitted into a steel cylinder mounted in an oak frame. The piston, connecting rod, thrust shaft, and guide bearing were all of aluminum. The piston had about two thousandths clearance in the cylinder when cold, and had no provision for sealing except the thermal expansion of the aluminum and oiling. The cylinder was five and one-half inches in diameter (corresponding to the inside diameter of the resonators) and eight inches long. The head end two inches of the cylinder was widened to six inches to receive the resonator tubing.

The basic resonator configuration, as the term is used in the text and tables, refers to the resonator configuration as described in this paragraph. Two sections of cylindrical, Lucite tubing ([illegible] inches long; 6.0 inches O.D., 5.5 inches I.D.) were butted together and cradled horizontally in three wooden supports

(see Figure 1). One end was inserted in the pulsator receiver station. The butted ends were sealed with Scotch tape which was easily removable. Small patches of the same material were used to seal orifices which were not in use. The overall length of the resonator, measured from the open end to the mean piston position (one-inch stroke), was found to be one hundred-seven and four-tenths inches, or nearly nine feet. The plastic tube ends were square-cut, and in particular, the edge of the open end of the resonator was square-cut or blunt. Eighteen orifices (0.070 in., drilled with sharp No. 50 drill) were spaced six inches apart, in a straight line along the upper surface. These were numbered as stations one through eighteen starting at the open end. The orifice near the open end was set in from the tube end by about 3/32 inches to permit attachment of fittings. Three additional orifices of the same diameter were drilled at stations 2, 7, 12, and 17. These, together with the top orifice, were given equidistant angular spacing (90° apart). The tube was carefully aligned with the axis of the pulsator piston. The resonator open end was eight feet from the facing wall and the resonator center axis was thirty-four inches from the floor.

The main modification to the basic resonator configuration, considered in this work, was that made to investigate the effect of a sharp versus a blunt open-end edge (Figure 5). This

was done by making a cylindrical tin collar two and one-half inches long which fit snugly inside the open end of the resonator. It was inserted one-half inch into the open end which increased the resonator length by two inches. Modeling clay was then applied to the outside of the tin collar to produce first the sharp, and then the blunt, open-end edge configuration. A pressure tap near the edge of the tin collar was numbered as station 14. A similar tin collar was used at the intersection of the tube sections for some flow visualization runs (Figure 10). It fit over the outside of the tubes and was two and one-half inches long so that it increased the tube length by one-half inch. It had one hole to admit a 1/16 inch OD probe, and another to admit a one-half inch duster spout. These holes were sealed with Scotch Tape when not in use.

Two identical plenum chambers were built (see Figures 1, 2). They were made from four inch galvanized rain spout and were fifty-one inches long. One of the four walls was flattened to permit the soldering on of flat plates (one-fourth inch thick), which were spaced [illegible] inches apart and tapped to receive ordinary one-eighth inch pipe (hex-head) fittings. A similar fitting was attached at each end. Rubber tubing (one-fourth inch ID, approximately thirty five inches long) was attached to each of the end fittings and connected to a T fitting,

(5/16 inch ID). Similar pieces of rubber tubing, approximately fifty-five inches long, were used for connecting the two Y fittings to liquid manometers when the plenum chamber was in use.

The manometers employed were of the liquid, draft gage type (Figure 1). The one which was used for all the traverse readings and with the plenum chamber and during the wall static measurements was a laboratory type using oil. The scale was calibrated, however, in inches of water. The range was zero to fifteen inches with only the zero to three inch part of the scale inclined. A small three inch-scale, draft manometer (inclined), filled with distilled water, was used with the plenum chamber against the open air, except for occasional readings at Sta. No. 1 which were off the scale. These manometers could be read to the third decimal place on the inclined scale and to the second decimal place on the vertical scale. All readings were taken as referred to atmospheric.

The pressure measurement instrumentation was of three types: (1) *wall static*, used for most of the measurements of mean static pressure at the resonator wall; (2) *internal traverse*, used for the mean static and total head pressure traverse measurements inside the resonator; (3) *external traverse*, used for traverse measurements in the jet.

The pull whistle configuration (Figure 2, B) consisted of the two planed sheathings and connectors arranged as shown in Figure 1. The [illegible] in resonator [illegible] [illegible]-less. A small iron tube was fitted over a piece of copper tubing; the tube was connected to the same [illegible] as the [illegible] of the resonator and was [illegible] inch long, [illegible] of [illegible] and three-quarters inches [illegible]. The copper tube, [illegible] was one-half inch long, five-sixteenths inches [illegible], and three-eighths inches [illegible]. The stop-cock fitted to the [illegible] had a straight, [illegible] bore, [illegible], [illegible] five-thirty-seconds inches [illegible], and [illegible] length. [illegible] [illegible] on the stop-cock [illegible] similar to a bell-[illegible], [illegible] [illegible] by [illegible] of [illegible]. The base fitting was [illegible] a rubber washer and a metal [illegible]. The base fitting with the copper tube was connected to the [illegible] by a piece of rubber tube [illegible] one-half inches long and [illegible]. [illegible] the distance between the [illegible] and the base fitting was approximately one-half inch [illegible] in position, [illegible] the [illegible] length of the [illegible] was only [illegible] of the copper tube. [illegible] the [illegible] length [illegible] from the [illegible] of the [illegible] to the [illegible] of the [illegible]

chamber was about three and three-fourths inches wide. Three different changes in hot area, namely, the radiator fitting, the copper tube and [illegible] connection fitting, and the flared.

A modification of the bell and flaring configuration was made at the [illegible] as shown in Figure [illegible]. This was done to permit the [illegible] connection needed in the installation of the [illegible] fitting, and [illegible], the main source of the large tube fitting used at the [illegible]. The [illegible] discharge, in this case, consisting of two lengths of brass tubing, which were soldered or [illegible] in place so that they were flush with the inside of the discharge wall. This brass tubing had an inside diameter of thirty-three thousandths, and an outside diameter of sixty-three thousandths. A similar piece of brass tubing was soldered into a [illegible], which was [illegible] in [illegible] fitting, a section of the [illegible] of the plane [illegible]. [illegible] of plastic, was [illegible] long, [illegible] this [illegible] tubing. The [illegible] of the [illegible] [illegible] [illegible] shown in Appendix as [illegible] 2.

The *internal transfer* [illegible]

arrangement as shown in Figure 3. A metal base plate, metal clamp, and a [illegible] were used to attach the fitting to the thermistor [illegible]. A brass fitting, normally used to attach copper tubing with a flared end to a one-eighth inch female pipe fitting, was modified by filling the inside bore with brass [illegible] and drilling two holes to the dimension required for the probe it was desired to use. The pressure cap for this fitting had a small, six-inch, steel scale (calibrated in sixty-fourths of an inch) mounted on its side and extending in a direction normal to the reference surface. The cap also had a small rubber washer inside it to provide an airtight seal at the probe. The probes were connected to the two-way stopcock on the plenum chamber by a six-inch piece of plastic tubing, [illegible] tubes inside the chamber. The various probes used with this equipment are described separately.

A description of the probes used with the internal traverse arrangement follows.

(1) A probe for the approximate measurement of static pressure was made from a hypodermic needle. The end was cut off squarely and polished so that if the probe axis were exactly normal to the flow direction, the flat end plane would be parallel to the flow and a static pressure reading would

be obtained. This probe was six inches long, twenty-two thousandths inches I.D., and thirty-four thousandths inches O.D.

(2) Another static probe similar to (1) was made from brass tubing. This probe was eight and one-half inches long, thirty-two thousandths inches I.D., and sixty-three thousandths inches O.D.

(3) A total head probe was made from brass tubing with the same dimensions as (2) except that it was six inches in length, overall. The end of this probe was again rounded to hemispheric shape, except that the end remained open. A one-eighth inch radius ninety-degree bend was made [illegible] inches from the end so that the plane of the opening was approximately one-half inch displaced from, and parallel to, the axis of the major portion of the probe. This has been referred to as an L-shaped total head tube because of its shape.

(4) A total head probe was made from brass tubing with the same dimensions as (2). In this case, the end was closed off with solder and polished down to the shape of a hemisphere. A hole was drilled in

the side of the probe three-sixteenths of an inch from the end. This hole was twenty-eight thousandths (0.028 in.) diameter which was only slightly different than the inside diameter of the probe (thirty-three thousandths). This probe has been referred to as a cylinder-type total head tube since it is based on the fact that stagnation occurs at the leading edge of a cylinder placed normal to a steady flow.

The external traverse configuration consisted of an arrangement as shown in Figure 6. The probe fitted snugly into a one inch bearing in a mounting plate on the support frame. It could be slid back and forth using a scribe mark calibration on the probe for positioning. Vertical positioning could be made by moving the mounting plate up and down between the two vertical support bars. When positioned vertically, the mounting plate position was fixed by a clamp arrangement. The vertical support bars could be rotated about a vertical axis providing another degree of freedom. The external traverse probes were connected to the plenum chamber by a six-inch piece of rubber tubing (3/16 in. ID) and a one-way stop-cock.

A description of the probes used with the internal traverse arrangement follows.

(a) A Kiel (total-head) tube (Ref. 14) with a flanged duct was available and this was used for all of the external total-head measurements. The sensing tube inside the outer shell of this probe had an inside diameter of approximately [illegible] of an inch and was approximately two inches in length. It led into a larger brass tube which also served as the support or probe shaft, the orientation of the Kiel tube being at a right angle to the shaft axis. The shaft was eighteen inches long, making about twenty inches overall, five thirty-seconds of an inch in inside diameter and three sixteenths of an inch outside diameter. The outer shell of the Kiel tube was one-quarter inch in outside diameter and its head was offset from the axis of the shaft by three-eighths of an inch.

(b) A static probe for use with the external survey arrangement was made, from brass tubing, into the shape of an L, where the short part was four inches long and the long part, which served as the probe shaft, was eighteen inches long. The probe had the same dimensions as the shaft of the Kiel

tube (5), but this was reduced at a point two inches short of the bend. From here on the smaller section of the tube was six inches in overall length, one-eighth of an inch in inside diameter. The end of the short part of the "L" was cut square and polished smooth so that, if its plane were placed exactly parallel to the flow, it would read purely the static pressure. It was used in this way, facing down, with the end plane lying in the horizontal plane of symmetry through the central axis of the stagnator and jet.

Various methods of producing smoke were tried. The most satisfactory method employed [illegible].

Quantities of a white, plastic, siliceous, insulating material, with the trade name Santocel (Monsanto Chemical Company), were available. This material is extremely light, with a fluffy crystalline texture. The finest particles have a very low free-fall rate. This was injected into the stagnator at the gas-control, by blowing it in with a large rubber [illegible] or by simply sprinkling a little along inside the tubes before the start of a run.

The flow pictures shown were taken using a [illegible]

light [illegible] with a firm [illegible] [illegible]. The [illegible] [illegible] [illegible] produced by tapping the [illegible] with a [illegible]-inch [illegible].

The approach [illegible] studied by [illegible] [illegible] [illegible] well but [illegible] [illegible] the general recommendations [illegible] pulsating flow measurements is contained in [illegible] /10/. [illegible] It is concluded that "the first resonant frequency of the pressure-measurement system should be kept well above the highest pressure frequency to be measured. This should be ideally be accomplished only by installing the pressure-sensing element as close to the point of measurement as possible." Thus, tube length for indicating pressure measurements must be kept as short as possible. With a liquid connected to the sensing instrument, [illegible] [illegible] [illegible] may be used to damp out the pulsations.

RESULTS AND DISCUSSION

Mean Static and Total Pressure Distribution Along the Resonator Axis of Symmetry

Values of mean static pressure, mean total pressure taken with the probe opening facing the piston, and mean total pressure taken with the probe opening facing away from the piston, are shown in Figures 7 and 8 for 3 piston strokes 5, 7, and inches. The highest pressure values occur near the piston and the lowest values occur just inside the resonator mouth. All values throughout most of the resonator, [illegible], referred to atmospheric, but rise sharply just outside the resonator.

The total heads taken facing in opposite directions, parallel to the axis, appear to show very little difference in the region near the piston (Figure 8). A tendency for the "facing-away" readings to be less than the "facing" readings becomes evident toward the resonator aperture. At a position about two inches inside the resonator, this trend is reversed, exhibiting marked divergence at the orifice plane. Another reversal just outside the resonator [illegible] and marks the transition to jet flow with the total head facing the piston being well above corresponding values of the total head facing away from the piston, indicating toward the static values of the [illegible] being smaller.

with increased internal distance from the open end of the resonator.

The reversal of measured total head values at the resonator mouth suggests that the air inflow and outflow is truly alternating over the whole open end, and that the air coming in has nearly atmospheric total pressure, since it is mostly drawn from the surrounding atmosphere at the inlet, and has experienced the dissipation associated with intense oscillations over a relatively short time. Rayleigh /4/ states, "the two effects (inflow and efflux of the air in a jet) are of course in reality alternating, and only appear to be simultaneous in consequence of the inability of the eye to follow such rapid changes".

The total head reversal, at a short axial distance inside the resonator open end, marks the transition point between the air movement inside the major portion of the resonator which appears to be primarily oscillatory, and the end vortex and jet flow which appears to be primarily an external circulation system strongly placed in the region of the resonator open end. Visual observations (Figure 2) suggested that much of the surrounding air, drawn towards the resonator open end, joined the jet flow from the periphery of the vortex system without

entering the resonator. It appeared that this air was [illegible] and [illegible] throughout the jet flow.

The maximum difference between static and total head values (approximately three and one-half inches of water) occurs just inside the resonator open end and are indicative of velocities on the order of one hundred twenty-five feet per second. The mean velocity at one foot outside the resonator is indicated as about eighty feet per second, and the mean velocity at a distance of three feet outside the resonator is indicated as about sixty feet per second. These values compare with the maximum sinusoidal piston velocity of eight and one-tenth feet per second for the 0.272 in. piston stroke.

Lateral Pressure Gradient

A comparison of the mean static pressure distribution along the wall of the resonator with the axial mean static pressure distribution is shown in Figure 8. The axial gradient is greater than the wall gradient such that considerably lower pressure values exist along the axis as the open end of the resonator is approached. The values are very nearly the same near the closed end. A sharp reversal of the static pressure trend occurs just inside the open end, which may be related to the effect of the edge vortex system. All divergence of the-

axial and wall static pressure distributions correlates with the visual observations of greatly increased dust particle path lengths near the open end, assuming that the latter are an indication of increased air molecule path lengths.

Profiles of mean static pressure distribution inside the resonator are shown in figures [illegible] 16. These profiles, with the exception of that for station One, were obtained by probing from two pairs of opposed directions at each station as a check upon the symmetry of the pressure distribution.

Profiles of mean static and total pressures in the external jet area (horizontal plane) are presented in figure 17 for distances one-half, two and one-half, and six inches from the open end of the resonator.

Total head profiles are presented in figure 18. Their gradients appear to be small except in the region near the open end of the resonator.

Variation in Mean Static Pressure Distribution with Piston Stroke

The mean static pressure distribution along the resonator wall for various magnitudes of piston stroke is shown in figure 9. The pressure gradient is greatly decreased with piston stroke, although the original pressure distribution pattern is

obtained. The cross plot of pressure versus piston stroke is shown in Figure 9. It appears that the variation is essentially linear in this range. This agrees with the trend of the torque versus piston stroke results presented in Ref. 1 for a straight resonator without end modification. The greatest rate of change is positive and is near the closed end, and the least rate of change is negative and is near the open end.

Variation in Pressure for a Flared and Sharp-Edged Open-end Resonator Configuration

The difference in wall static mean pressure distributions for resonators with flared and sharp edged open-end resonator configurations is shown in Figure 10. Somewhat lower values were obtained with the tapered edge.

Variation in Wall Mean Static Pressure with Frequency for Fixed Resonator Length

The variation of mean static pressure distribution along the resonator wall is shown in Figure 11 for various pulsator rpm values. A cross plot of pressure versus rpm for selected stations is shown in Figure 12. It is evident that a longitudinal pressure gradient is produced which has the greatest

value of the resonant frequency; and that this quantity is such that the maximum tends to occur at, or near, the closed end (piston). The minimum values occur at, or near, the open end. This is in agreement with theory (Ref /5/). Response at plate has been used to determine the resonant frequency of the basic standard configuration in figure 11, and for the open-end slot modification in figure 13. The resonant peak for the basic configuration was taken as 1405, and resonant peak for the modified configuration was taken as 1480. The theoretical formula (Equation 1) gave values of 1500 and 1550, respectively.

The response curves all curves show a definite difference in the slope on either side of the peak. The positive slope flattens out as resonance is approached while the negative slope drops off much more rapidly. A jump in reading of pressure at the peak reflects the instability associated with the resonance in this range. The results probably are obtained by operating one of these into the peak on the low side. It may be noted that the general shape of the pressure versus frequency curve, Figure 11, which was plotted for the highest pressure curves presented in this report.

Thrust Values

Using mean static pressure values from [illegible], and assuming that the [illegible] pressure at the [illegible] was atmospheric, values of thrust were calculated for various values of [illegible] pressure. These values are plotted in Figure 15. [illegible] shown in Figure 6. [illegible] Ref. 1, [illegible].

The maximum value of thrust [illegible] for the [illegible] pressure of [illegible] and the [illegible] length [illegible] in. [illegible]. The value for [illegible] length. This compares [illegible] values of thrust [illegible] for a similar [illegible] (Ref. 1), [illegible] pressure.

[illegible]

[illegible] (Figure 19), [illegible] by early investigators [illegible], were [illegible] evident at [illegible] (0.054 in.). It [illegible] difficult to produce the [illegible]

figures with increased piston-stroke up to one inch. Instead, with the introduction of sufficient quantities of ink, the tendency was for one large, well-defined figure to form along the cylinder axis and persist. This large figure was clearly affected or distorted by the presence of the pulsating jet orifice. The jet rings at [illegible] persisted, however, without much change in spacing. The jet rings became larger and more irregular (Figure 20) with increased piston stroke magnitude.

Diffusion of both small and large quantities of ink was extremely rapid at large amplitudes of piston stroke making detail observation difficult, but surveying in these turbulent areas was possible with large pulsation amplitudes. The distribution of large quantities of dye, introduced directly into the resonator, appeared to be by random diffusion at a uniform rate associated with the degree of turbulence present, and apparently little affected by patterns of general circulation within the resonator such as has been suggested ([illegible] /6/). A strong circulation was associated with the jet flow, but this effect appeared to be mainly concerned with only relatively shallow primary penetration of the resonator as shown in Figure 22 for low piston stroke amplitude.

A comparison of the depth of penetration of the same vortex system with small and large piston stroke magnitudes is presented in Figures 25 and 26. The estimated increase in penetration with increased piston stroke magnitude is plotted in Figure 27 from these and other observations.

Small particles oscillating or vibrating back and forth in a straight line appear to the eye as straight lines if the pulsation is fast enough. The observation of fine, individual, suspended particles of dust or lint inside the resonator was quite readily made. The best observations were possible when only a few, fine particles were present so that interference between particles was negligible. The dust particles described straight paths which were usually parallel to the axis throughout the resonator, excluding the small region penetrated by the jet vortex system. The location of these particle paths seemed to be stationary, with the greatest visibility evident near the closed (piston) end. Observations were made in which such suspended particles did not change location significantly for several minutes, even within a foot of the open end. Small external disturbances, such as would be caused by a person walking about near the resonator or the opening of a door, were sufficient to disturb the equilibrium of the particles within the resonator such that a slow, irregular relocation occurred.

A nearby open window was sometimes sufficient to cause continuous disturbances such that only the particles near the closed end remained relatively unaffected.

The magnitude of the dust particle paths (Figures 28 and 29) observed was seen to be much greater near the open end than near the closed (piston) end. For a given location, the magnitude of the particle paths observed was seen to increase with increase of piston stroke. Some visual estimations of dust particle path length were recorded (Table XII) and plotted in Figure 31. It is difficult to make such estimations accurately and these results must be regarded with caution.

Detailed observations of the dust figures were made in the hope that their behavior, although apparently an incidental phenomenon, might shed additional light on the fundamental nature of the acoustic jet. Figure 26 is a close-up photograph of one of these lateral figures which, unfortunately, does not reveal the significant detail, and it is observable that each this ridge is made up of tiny particles describing circles, with lines parallel to the axis. Incidentally, when looking at the dust figure against the light, it is clear or [illegible] central plane. The spacing of the dust figures is somewhat regular (Figure 30), but irregularities are usually present. The format-

tion of dust figures was observed as a sort of sudden growth from a lateral dust ridge at the bottom of the tube. There were usually several of these dust ridges between dust figures. When a board was clamped over the open end of the resonator, thus closing it, the dust figures all collapsed into dust ridges. They collapsed also if a large orifice was opened near the middle of the resonator allowing the pressure to escape. Dust figures were occasionally observed to collapse during operation, as a sort of reversal of the growth process. The width of dust figures one foot inside the resonator open end was observed to be about one and one-half inches which is, significantly, about twice the observed particle path length observed at the same location. This observation was for a particle diameter of [illegible] inches. The same relation between dust figure width and particle path length was observed to exist wherever dust figures were formed.

The rate of longitudinal movement was greatest near the open end. Observations, taken with a [illegible] inch [illegible] strip, showed the average rate near the open end (station [illegible]) to be about three-tenths foot per second; the average rate at one-third the tube length from the open end was two-tenths foot per second; and the movement at two-thirds the tube length from the open end was negligible, although it appeared that [illegible]

condition was stationary. Dust fibres, arriving at the open end of the resonator, would fill the resonator cavity and feed out the central jet. This produces an excellent means of visualizing the low piston stroke flow pattern of the jet as shown in Figures 21, 22, and 23, and shows the degree of symmetry in the flow.

Limitation of Results

The main factor affecting the results obtained was the instrumentation detail with reference to the diameter and length of all tubes and constrictions used in the pressure measurement system. Quantitative evaluation of the data would depend on detailed calculation of the system losses along the lines presented in the discussion of related theory (Refs. 13, 11, 16).

It was found that a basic requirement was the exercise of extreme care with regard to the uniformity of the test equipment at each station. During the course of the investigation, some experimental errors were discovered.

Good reproducibility of results was experienced. The results did not appear to be sensitive to the small variation

in ambient conditions experimented.

The basic assumptions involved in the transient investigation were that the flow was axially symmetrical, and that the main components of flow were parallel to the axis. The former seems justified by a reasonable regularity of the flow visualization results, and the foregoing, [illegible] investigations. The latter appears generally valid except within the area in the arc, or between the arc electrodes and the jet. Beyond this region, it appears generally valid along the axis of symmetry.

The general conclusions reached through the flow visualization [illegible] are believed to be valid, although not fully supported by photographs. Part of the phenomena [illegible] with the [illegible] with the pressure distribution. The observations of the dust particle path lengths and [illegible] [illegible] should be regarded as qualitative, involving [illegible] of small linear dimensions. Also, the dust particle lengths were a function of the dust particle mass.

CONCLUSIONS

These conclusions hold strictly for a single resonator and pulsator configuration and are not intended as absolute generalizations.

(1) It is possible to produce a significant mean pressure gradient in the axial and lateral directions, in a resonator closed at one end and containing air, by pulsating a plate at the closed end.

(2) The longitudinal mean pressure gradient has its maximum value near the theoretical resonant frequency of the resonator with corrections for end effects.

(3) The mean pressure distribution and overall flow pattern has axial symmetry to the major degree.

(4) The longitudinal mean pressure gradient increases with amplitude of pulsator vibration and that pressure values near the closed end increase positively and values near the open end increase negatively.

(5) The rate of change of mean static pressure, with amplitude of pulsator vibration, is greater near the closed end; lesser near the open end; and is essentially linear for any

piston position along the resonator wall.

(6) The lateral mean static pressure gradient over the major portion of the resonator, showed that the highest pressures occur near the wall. This gradient approaches zero near the closed end and is the greatest near the open end. A strong vortical nature of the mean flow is indicated, showing the influence of the strong generated vortex.

(7) The greatest values of mean velocity along the axis, as indicated by mean static and total pressure measurements, occur at, or just inside, the resonator open end.

(8) The primary aspect of the air movement inside the major portion of the resonator appears to be a longitudinal oscillation in the direction paralleling the axis of symmetry. There appears to be superposition which contains changes in that particle path length such that the largest amplitude of particle vibration occur near the resonator wall and increased amplitude of particle vibration occur with increased amplitude of pulsating velocity.

(9) Near the resonant frequency, there is a pulsating vortex ring of air centered at the open end edge of the resonator which would appear to alternate with a pulsating bubble,

line of stagnation source and sink. This appears to be mainly an external-circulation effect [illegible] [illegible] [illegible], in the open end [illegible] conditions [illegible] the vibrating gas column inside the resonator. In cross-section, it appears to be initially symmetrical, relatively shallow, U-shaped, [illegible] [illegible] acting as the [illegible] source of a jet efflux. The apparent depth, to which the gas should appear penetrating the resonator, increases with amplitude of pulsator vibration, but remains relatively shallow.

(10) With increased amplitude of pulsator vibration, the vibrating gas column inside the resonator appears to become increasingly turbulent.

BIBLIOGRAPHY

1. [illegible]: "First Interim Report on the Investigation of Intermittent Flow," Report No. [illegible], United Aircraft Corporation, East Hartford, Conn., [illegible] September, 1949.

2. [illegible]: "Relation Between Acoustic Phenomena and Dynamic Thrust," Master of Science Thesis, Aeronautical Engineering, University of Minnesota, August 1950.

3. Logan, Joseph G., Jr.: "Suggested Forms of Air Duct Motors Utilizing Intermittent Combustion," Parts I and II, Project Squid, Tech. Memo. No. CAL-17, Cornell Aeronautical Laboratory, Inc., Buffalo 21, New York, 28 February, 1949.

4. Rudinger, George and [illegible], Edward J.: "The Construction of Wave Diagrams for the Study of One-Dimensional Non-Steady Gas Flow," Technical Memorandum No. CAL-14, Project Squid, Cornell Aeronautical Laboratory, Inc., Buffalo 21, New York, 10 March, 1949.

5. Rudinger, G., Logan, J., and [illegible]: "Investigations of Acoustic Jets," (a) Part I, Report No. CAL-15, (b) Part II, Report No. CAL-19; Project Squid, Cornell Aeronautical Laboratory, Inc., Buffalo 21, New York, 10 March, 1949.

6. Rayleigh, John W. S.: "The Theory of Sound," Vol. I, Dover Publications, New York, 1945.

7. Morse, Philip M.: "Vibration and Sound," McGraw-Hill Book Co., Inc., 1936.

8. Ingard, U.: "On the Radiation of Sound into a Circular Tube, with an Application to Resonators," Acta Polytech. 20 (Elect. Eng. Ser. 1, No. 3) Trans. Chalmers Univ. Tech. Gothenburg 70, 3-[illegible] (1948). In English. The case of a plane piston source in rigid tube is treated theoretically.

9. Wood, A. B.: "Textbook of Sound," G. Bell and Sons, Ltd., 1930.

10. Liston, J.: "Aircraft Engine Design;" McGraw-Hill Book Co., New York, 1942.

11. Iberall, A. S.: "Attenuation of Oscillatory Pressures in Instrument Lines;" Transactions of the ASME, Vol. 72, No. 5; July, 1950.

12. Taback, Israel. "The Response of Pressure Measuring Systems to Oscillating Pressures;" NACA TN 1819, February, 1949.

13. [illegible], J.: Physical Review, 75, [illegible], 194[illegible].

14. Pope, Alan. "Wind-Tunnel Testing;" John Wiley and Sons, Inc., New York, 1952.

15. Liepmann, H. W., Puckett, A. E.: "Aerodynamics of a Compressible Fluid;" John Wiley and Sons, Inc., New York, 1949.

16. Wildhack, W. A.: "Pressure Drop in Tubing in Aircraft Instrument Installations;" NACA TN 593; Wash.; February, 1937.

TABLE I

DETERMINATION OF RESONANT FREQUENCY FOR *BASIC RESONATOR CONFIGURATIONS**

(Resonator Wall Mean Static Pressure Data)

Instrumentation: *Wall Static   Piston stroke: 0.272 in.
End Edge Shape: Square   Resonator Length: 107.1 in.

Sta. No.			6	10
X (in. from open end)			60	102
RPM	H_a	t	h_s	h_s
1854	29.24	82	-1.82	17.25
1858	29.24	82	-1.81	5.12
1867	29.24	82	-2.01	5.77
1874	29.24	83	-2.04	5.80
1879	29.24	85		6.15
1884	29.24	82	-2.12	6.15
1892	29.24	82	-2.17	5.30
1898	29.24	85		6.38
1901	29.24	83	-2.11	6.10
1905	29.24	85		6.40
1911	29.24	85		6.45
1914	29.24	82	-2.00	6.21
1916	29.24	82	-2.05	6.18
1925	29.24	85		5.95
1940	29.24	83	-1.90	5.90
1961	29.24	82	-1.57	4.90
1970	29.24	85	-1.72	11.00

*See Apparatus and Nomenclature

**See Limitations

TABLE 11

DETERMINATION OF RESONANCE RPM FOR SHARP END

RESONATOR CONFIGURATION*

(Resonator Wall Mean Static Pressure Data)

Instrumentation: Small Static   Piston Stroke: 0.372 in.

Sta. No.	16	18
x	0	10
H_a	29.90	29.90
t	80	80
L	102.4	102.4
End Edge Shape	Sharp	Sharp
RPM	h_s	h_s
1795	-2.25	10.20
1800	-2.55	5.70
1808	-2.51	3.50
1813	-2.67	3.70
1820	-2.87	3.72
1828	-2.97	3.90
1836	-3.02	4.10
1843	-3.10	4.20
1852	-3.21	4.35
1860	-3.05	4.40
1864	-3.05	4.35
1867	-3.09	4.42
1875	-3.00	4.12
1884	-2.88	5.28
1890	-2.60	5.70
1904	-2.52	6.12
1908	-2.45	7.41
1917	-2.25	17.10

*See Apparatus and Nomenclature

**See Limitations

TABLE III

VARIATION OF RESONATOR WALL MEAN STATIC PRESSURE WITH FREQUENCY

Instrumentation: Wall Static Piston Stroke: 0.[illegible] in.
End Edge Shape: Square Resonator Length: 107.[illegible] in.
Resonator: Basic Configuration

CPS*		1948	1970	1990	1903	1916	1925	1930	1921
P_a		29.24	29.22	29.27	29.24	29.24	29.22	29.24	29.24
t		80	88	85	80	82	88	80	80
Sta. No.	x	h_s	h_s	h_s	h_s	h_s	h_s	h_s	h_s***
1	0	-2.46	-3.08	-3.27	[illegible]	-5.42	-3.20	[illegible]	[illegible]
2	6	-1.76	-2.27	-2.41	-2.05	[illegible]	-2.20	[illegible]	[illegible]
3	12	-1.78	-2.21	-2.07	[illegible]	-2.21	-2.21	[illegible]	-2.18
4	18	-1.55	-1.90	-1.20	-2.13	-3.30	-1.93	-1.75	[illegible]
5	24	-1.32	-1.58	-1.46	-1.60	-1.14	-1.44	-1.75	-1.12
6	30	-1.63	-1.90	-2.14	-2.02	-2.08	[illegible]	-1.70	[illegible]
7	36	[illegible]	-1.20	-1.11	-1.73	-1.34	-1.73	-1.28	
8	42	-0.17	-0.19	-0.70	-0.40	-0.05	-0.50	-0.77	[illegible]
9	48	+0.14	-0.08	+0.05	+0.01	0.00	+0.02	[illegible]	
10	54	1.07	+1.11	1.19	1.08	+0.97	+0.90	+0.91	
11	60	1.90	[illegible]	[illegible]	[illegible]	2.17	2.12	2.09	+2.40
12	66	2.15	[illegible]	2.85	[illegible]	2.22	2.41	2.21	
13	72	[illegible]	[illegible]	[illegible]	[illegible]	[illegible]	[illegible]	[illegible]	[illegible]
14	78	[illegible]	[illegible]	[illegible]	[illegible]	[illegible]	[illegible]	[illegible]	
15	84	[illegible]	[illegible]	[illegible]	[illegible]	[illegible]	[illegible]	[illegible]	[illegible]
16	90	[illegible]	[illegible]	[illegible]	[illegible]	[illegible]	[illegible]	[illegible]	[illegible]
17	96	[illegible]	[illegible]	[illegible]	[illegible]	[illegible]	[illegible]	[illegible]	
18	102	[illegible]	[illegible]	[illegible]	[illegible]	[illegible]	[illegible]	[illegible]	[illegible]

*See Appendix and Nomenclature

**See Limitations

***Modified connection (small tube) at station number [illegible]
(See Figure 8)

TABLE IV

RESONATOR WALL MEAN STATIC PRESSURE DATA,

SHOWING EFFECT OF END LIP SHAPE*

Instrumentation: Small Static Modified
Piston Stroke: 0.979 in.
Resonator Length: 100.4 in.
Resonator: **Basic Configuration plus Modified End

End Edge Shape		Sharp	Sharp	Square
H_b		29.27	29.59	29.81
t		86	85	85
RPM		1801	1801	1801
Sta. No.	x	h_s	h_s	h_s
1a	0	-3.00	-2.10	-2.94
1	3	-3.00		-2.72
2	8	-2.51		-2.55
3	14	-2.11		-1.57
4	20	-2.12	-2.17	-1.05
5	26	-1.76		-1.47
6	32	-2.12	-2.18	-1.04
7	38	-1.68		-1.54
8	44	-0.82		-0.50
9	50	-0.57	-0.02	-0.12
10	56	+0.42		+1.11
11	62	1.60		2.63
12	68	1.80	+1.00	2.81
13	74	2.09		3.50
14	80	2.15		3.37
15	86	3.14	1.37	1.63
16	92	2.50		3.26
17	98	1.90		7.20
18	104	+1.22	+1.82	+2.51

*See Apparatus and Nomenclature

**See Limitations

TABLE V

RESONATOR WALL MEAN STATIC PRESSURE SURVEY

WITH VARIABLE PISTON STROKE**

Instrumentation: Wall Static   Resonator: *Basic Configuration
End Edge Shape: Square   Resonator Length: 107.4 in.

Piston Stroke, in.		0.051	0.292	0.512	0.722	0.970
RPM		1306	1306	1302	1305	1302
H_a		29.42	29.42	29.42	29.42	29.42
t		83	83	83	83	83
Sta. No.	x	h_s	h_s	h_s	h_s	h_s
1	0	-0.13	-0.65	-1.04	-1.71	-2.31
2	6	-0.09	-0.60	-1.16	-1.69	-2.15
3	12	-0.06	-0.57	-1.20	-1.75	-2.31
4	18	-0.02	-0.54	-1.19	-1.71	-2.26
5	24	±0.03	-0.72	-1.01	-1.18	-1.66
6	30	-0.03	-0.77	-1.27	-1.63	-2.13
7	36	-0.03	-0.70	-0.98	-1.51	-1.53
8	42	±0.03	-0.11	-0.50	-0.76	-0.63
9	48	0.07	±0.02	±0.08	±0.03	±0.02
10	54	0.12	0.35	0.63	0.73	0.59
11	60	0.19	0.65	1.03	1.34	1.62
12	66	0.22	0.90	1.36	1.60	2.16
13	72	0.21	1.09	1.90	2.52	3.26
14	78	0.20	1.31	2.08	3.29	4.30
15	84	0.22	1.40	2.79	3.70	4.99
16	90	0.10	1.06	3.11	3.21	2.60
17	96	0.33	1.01	3.79	3.21	2.21
18	102	±0.32	±1.11	±3.71	±3.12	±2.60

*See Apparatus and Nomenclature

**See Limitations

TABLE VI

CALCULATED THRUST VALUES

(Pressure Data from Figure 8 and Table V)

t	V_a	p_g (at piston)	p_g (at open end)	F (lbs)
0.278	27.14	16.6	-6.3	4.1
0.762	28.11	15.1	-2.7	6.0
0.342	26.21	15.7	-2.1	4.5
0.292	26.24	11.6	-0.6	2.1
0.351	27.24	10.6	-0.1	0.8

TABLE VII

FOUR-WAY, [illegible] RADIAL [illegible], [illegible] DATA*

Instrumentation: [illegible] traverse (Probe 2)   Piston stroke: [illegible] in.   [illegible] Square
Generator: *Basic configuration   [illegible] length: 107.0 cm.

Run No.	[illegible]	[illegible]	[illegible]	[illegible]	7	7	7	7	12	12	[illegible]	[illegible]	17	17	17	17
[illegible]	1001	1001	1002	1002	1002	1002	1002	[illegible]	[illegible]	[illegible]	[illegible]	1001	1001	1001	1002	[illegible]
[illegible]	22.17	[illegible]	[illegible]	[illegible]	[illegible]	[illegible]	[illegible]	[illegible]	[illegible]	[illegible]	[illegible]	[illegible]	[illegible]	[illegible]	[illegible]	[illegible]
[illegible]	84	84	84	84	84	84	84	84	84	84	84	84	85	85	85	85
φ***	0°	180°	90°	270°	0°	180°	90°	270°	0	180	90	270°	0°	180°	90°	270°
[illegible]	[illegible]	[illegible]	[illegible]	[illegible]	[illegible]	[illegible]	[illegible]	[illegible]	[illegible]	[illegible]	[illegible]	[illegible]	[illegible]	[illegible]	[illegible]	[illegible]
0	-1.50		-1.72		[illegible]		[illegible]		[illegible]		[illegible]		[illegible]	[illegible]	[illegible]	[illegible]
0.25	[illegible]	-3.01	[illegible]	-4.02	-0.37	-1.46	[illegible]	-1.45	3.00	[illegible]	[illegible]	[illegible]	[illegible]	[illegible]	[illegible]	[illegible]
0.75	[illegible]	-4.20	-4.00	-1.28	-1.74	-1.44	[illegible]	[illegible]	[illegible]	[illegible]	[illegible]	[illegible]	[illegible]	[illegible]	[illegible]	[illegible]
1.25	[illegible]	-1.20							[illegible]	[illegible]			[illegible]	[illegible]		
1.75	-4.30	[illegible]	[illegible]	[illegible]	[illegible]	[illegible]	-1.50	[illegible]	3.01	[illegible]	[illegible]	[illegible]	[illegible]	[illegible]	[illegible]	[illegible]
2.25	[illegible]	[illegible]							[illegible]	[illegible]			[illegible]	[illegible]	[illegible]	[illegible]
2.75	[illegible]	[illegible]	[illegible]	[illegible]	[illegible]	[illegible]	[illegible]	[illegible]	[illegible]	[illegible]	[illegible]	[illegible]	[illegible]	[illegible]	[illegible]	[illegible]
[illegible]	[illegible]	[illegible]							[illegible]	[illegible]			[illegible]	[illegible]	[illegible]	[illegible]
1.75	[illegible]	[illegible]	[illegible]	[illegible]	[illegible]	[illegible]	[illegible]	[illegible]	[illegible]	[illegible]	[illegible]	[illegible]	[illegible]	[illegible]	[illegible]	[illegible]
1.25	[illegible]	[illegible]							[illegible]	[illegible]			[illegible]	[illegible]		
0.75	[illegible]	[illegible]	[illegible]	-1.20	[illegible]	[illegible]	[illegible]	[illegible]	[illegible]	[illegible]	[illegible]	[illegible]	[illegible]	[illegible]	[illegible]	[illegible]
0.25	[illegible]	[illegible]	[illegible]	[illegible]	[illegible]	-0.97	[illegible]	[illegible]	[illegible]	[illegible]	[illegible]	[illegible]	[illegible]	[illegible]	[illegible]	[illegible]
0		[illegible]		-1.71		[illegible]		[illegible]		[illegible]		[illegible]		[illegible]		[illegible]

*See Apparatus and Nomenclature
**See Illustrations
***Refers to angular position of probe introduction. See Nomenclature

TABLE VIII

ONE-WAY, INTERNAL RADIAL TRAVERSE, MEAN STATIC PRESSURE DATA**

Instrumentation: *Internal traverse (Probe 2)
Resonator: *Basic configuration
Resonator length: 107.4 in.

Piston Stroke: 0.978 in.
End Edge Shape: Square

Sta. No.	1	3	4	5	6	8	9	10	11	13	14	15	16	18
RPM	1000	1002	1000	1001	1002	1002	1002	1000	1002	1002	1002	1001	1001	1002
P_a	29.03	29.26	29.06	29.06	29.06	29.26	29.26	29.03	29.26	29.26	29.26	29.06	29.06	29.26
t	85	82	85	85	85	82	82	85	82	82	82	85	85	82
θ***	0°	0°	0°	0°	0°	0°	0°	0°	0°	0°	0°	0°	0°	0°
r^1	h_s	h_s	h_s	h_s	h_s	h_s	h_s	h_s	h_s	h_s	h_s	h_s	h_s	h_s
0	-4.39	-1.74	-1.[illegible]	-0.77	-0.11	+0.77	+1.[illegible]	+1.90	+2.77	+3.77	+4.20	+4.27	+5.52	+5.75
0.25	-5.92		-2.50	-2.25	-1.22			1.16				4.30	5.23	
0.75	-5.92		-7.25	-2.37	-2.15			1.03				4.75	5.24	
1.25	-4.52													
1.75	-7.90		-3.16	-2.25	-2.15			1.12				4.71	5.20	
2.25														
2.75	-8.4[illegible]	-4.[illegible]	-5.25	-2.99	-2.17	-0.76	+0.19	1.14	+1.77	+2.55	+4.1[illegible]	4.[illegible]	[illegible].24	+5.75
2.25														
1.75	-7.[illegible]		-3.25	-2.92	-2.1[illegible]			1.1[illegible]				4.92	5.22	
1.25	-5.92													
0.75	-4.89		-7.29	-3.00	-2.10			1.12				4.90	5.15	
0.25	-5.72		-6.29	-3.0[illegible]	-2.13			+1.20				+4.90	+5.10	
0														

*See Apparatus and Notation.
**See Limitations.
***Refers to roll position of probe introduction. See Nomenclature.

TABLE II

ONE-HALF, INTERNAL RADIAL TRAVERSE, HEAD TOTAL PRESSURE DATA*

Instrumentation: *Internal Traverse   Piston Stroke: 0.375 in.
Resonator: *Basic Configuration   End Edge Shape: Square
Resonator Length: 107.4 in.

Std. No.	2	3	13	10	17
RPM	1002	1002	1002	1897	1002
P_a	29.47	29.62	29.62	29.30	29.62
T	80	83	83	82	83
ϕ***	0°	0°	0°	0°	0°
Type of Probe	L-head-3	L-head-3	L-head-1	Cyl.-4	L-head-3

Probe Opening Facing Toward Piston:

r^1	h_o	h_o	h_o	h_o	h_o
0.25	-0.51	-0.25	+0.17	+2.49	+3.27
0.75	-0.41	-0.43	0.15	2.45	3.30
1.75	-0.49	-0.40	0.19	2.48	3.40
2.75	-0.53	-0.51	0.17	2.48	3.43
1.75	-0.44	-0.49	+0.19	+2.41	+3.45

Probe Opening Facing Away from Piston:

r^1	h_o	h_o	h_o	h_o	h_o
0.25	-0.55	-0.52	+2.58	+2.49	+3.37
0.75	-0.56	-0.55	2.59	2.46	3.27
1.75	-0.54	-0.39	2.62	2.35	3.29
2.75	-0.40	-0.41	2.65	2.35	3.23
1.75	-0.55	-0.35	+2.65	+2.54	+3.32

*See Apparatus and Nomenclature.

**See Limitations.

***Refers to wall position of probe introduction. See Nomenclature.

TABLE X

MEAN TOTAL PRESSURE SURVEY ALONG [illegible]

Instrumentation: *Internal traverse, cylinder Probe (1)
Resonator: *Basic configuration   Piston Stroke: 0.970 in.
Resonator Length: 107.4 in.   End Edge Shape: Square

Distance from tube wall, in. (r^1)		2.75	2.75
X_u		20.25	20.25
f_o		22	22
ϕ***		90	90
Probe Opening Orientation		Facing Piston	Away from Piston
Stn. No.	RPM	P_o	P_o
1	1902	-1.41	-0.07
2	1902	-1.50	-0.06
3	1901	-0.80	-0.17
4	1900	-0.56	-0.22
5	1903	-0.75	-0.45
6	1900	±0.00	-0.20
7	1903	0.62	±0.70
8	1901	1.11	0.97
9	1903	1.40	1.74
10	1897	2.50	2.40
11	1902	3.10	2.75
12	1901	3.60	3.50
13	1902	4.35	4.70
14	1902	5.10	5.10
15	1903	5.50	5.71
16	1902	5.90	5.92
17	1902	6.25	6.25
18	1901	6.45	±6.45

*See Apparatus and Nomenclature.

**See Limitations.

***Refers to wall position of probe introduction. See Nomenclature.

TABLE XIa

LATERAL MEAN PRESSURE DATA**

(Traverse in Horizontal Axial Plane)

Instrumentation: *External traverse   Piston stroke: 0.??? in.
Resonator: *Basic configuration   Open end cage: Square
Resonator Length: 107.4 in.

[illegible]	0.5	0.5	0.5	2.5	2.5	2.5
RPM	1001	1001	1001	1001	1001	1001
P_a	29.42	29.42	29.42	29.42	29.42	29.42
t	84	84	84	84	84	84
Type of Probe*	(5)	(5)	(6)	(5)	(5)	(6)
ϕ***	90°	90°	90°	90°	90°	90°
r	h_o(in)#	h_o(out)#	h_s	h_o(in)	h_o(out)	h_s
-4.0	-0.09	-0.25		-0.08	-0.23	
-3.5	-0.24	-0.41	-0.52			
-3.0	-1.05	-0.45	-0.97	+0.30	-0.43	-0.90
-2.5	-1.30	-0.64	-2.28			
-2.0	-0.50	-0.41	-2.10	0.71	-0.21	-0.29
-1.5	-0.13	-0.41	-1.70			
-1.0	-0.70	-0.25	-1.97	0.72	-0.12	-0.50
-0.5	-0.20	-0.29	-1.90			
0.0	-0.34	-0.13	-1.85	0.27	-0.12	-0.60
+0.5	-0.25	-0.20	-1.84			
1.0	-0.57	-0.74	-2.77	0.95	-0.29	-0.90
1.5	-0.47	-0.41	-2.50			
2.0	-0.71	-0.74	-2.99	1.14	-0.50	-1.10
2.5			-2.10			
3.0	-0.37	-0.75	-0.20	+0.75	-0.40	-0.70
3.5			-0.19			
4.0			-0.14			
5.0			-0.09	-0.08	-0.14	-0.14
6.0			-0.08			-0.05
7.0						-0.02

*See Apparatus and Nomenclature.
**See Limitations.
***Refers to wall position or direction of probe introduction, "r" is positive on side from which probe is introduced. See Nomenclature.
#Total head opening faces towards the piston (in) or away from the piston (out).

TABLE [illegible]

[illegible]

([illegible])

Instrumentation: [illegible]   Piston Stroke: [illegible]
Resonator: Plastic configuration   Open End Edge: Square
Resonator Length: 107.4 in.

Run		1921	1921	1921
H_d		[illegible]	[illegible]	[illegible]
L		[illegible]	[illegible]	[illegible]
Type of Probe		([illegible])	([illegible])	([illegible])
ψ		[illegible]	[illegible]	[illegible]
X	Y	h_0(in)„	h_0(out)„	h_s
-4.0	0	+0.76	-0.17	-0.50
-3.0	0	0.[illegible]	-0.[illegible]	-0.48
-2.0	0	0.61	-0.15	-0.[illegible]
-1.0	0	0.7[illegible]	-0.02	-0.62
0.0	0	0.71	-0.11	-0.62
+1.0	0	[illegible]	-0.15	-0.70
2.0	0	0.28	-0.21	-0.[illegible]
3.0	0	0.7[illegible]	-0.[illegible]	-0.[illegible]
4.0	0	0.10	-0.40	-0.[illegible]
5.0	0	+0.10	+0.[illegible]	-0.55
10.0	0	-0.15	-0.10	-0.[illegible]
0.0	12	+0.07		-0.5[illegible]
0.0	1[illegible]	0.[illegible]		-0.[illegible]
0.0	[illegible]	0.72		-0.[illegible]
0.0	30	0.77		-0.55
0.0	[illegible]	0.55		-0.71
0.0	[illegible]	+0.21		-0.90

*See Apparatus and [illegible].
**See Illustration.
***Refers to wall position or direction of probe introduction, "+" is positive to side from which probe is introduced. See Nomenclature.
„Total head opening faced towards the piston (in) or away from the piston (out).

TABLE XII

[illegible]

Piston Stroke, in.	Depth of Observed Penetration, in.	As Noted from
0.094	1.5	Visual Observation
0.094	1.5	Photograph (see Figs. [illegible])
[illegible]	[illegible]	Visual Observation
[illegible]	[illegible]	Visual Observation
[illegible]	11.0	Photograph (see Figure [illegible])
[illegible]	[illegible]	Visual Observation

Piston Stroke, in.	*Observed Particle Path Length, in.			
	Sta. [illegible]	Sta. [illegible]	Sta. [illegible]	Sta. [illegible]
0.094	[illegible]	0.5	0.2	0.1
[illegible]	[illegible]			0.1
[illegible]	[illegible]			[illegible]
[illegible]	Observation uncertain			
[illegible]	Observation uncertain			

*Note: Particle path observations were based on readily visible particles [illegible] of considerable mass, [illegible] also arrived at by watching the vibrating particles [illegible] appeared as straight lines. Consequently this data should be regarded as qualitative.

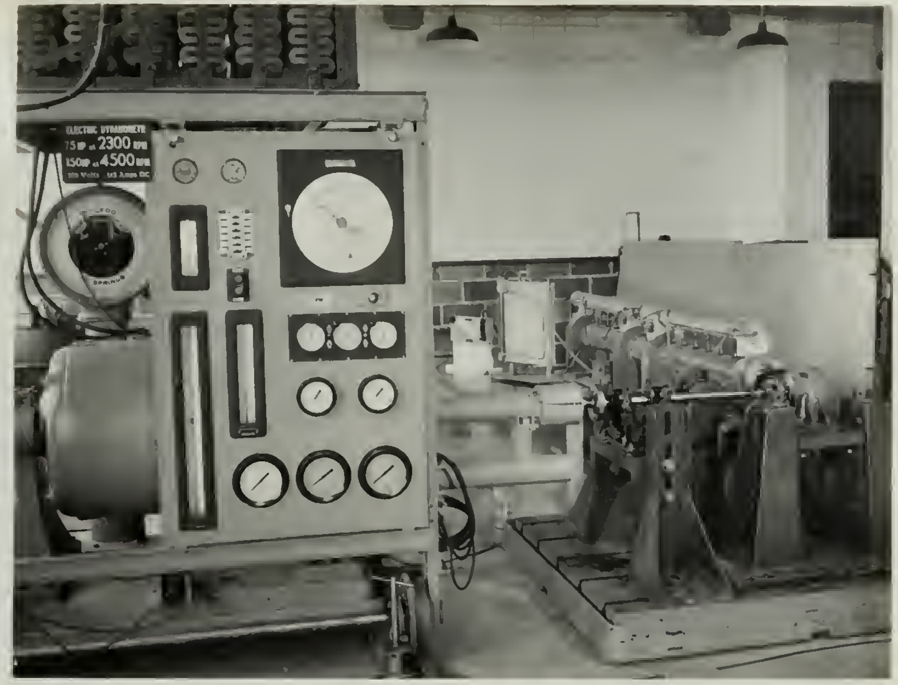
ELECTRIC DYNAMOMETER
75 HP at 2300 RPM
150 HP at 4500 RPM
Volts Amps DC

Figure 1 [illegible]

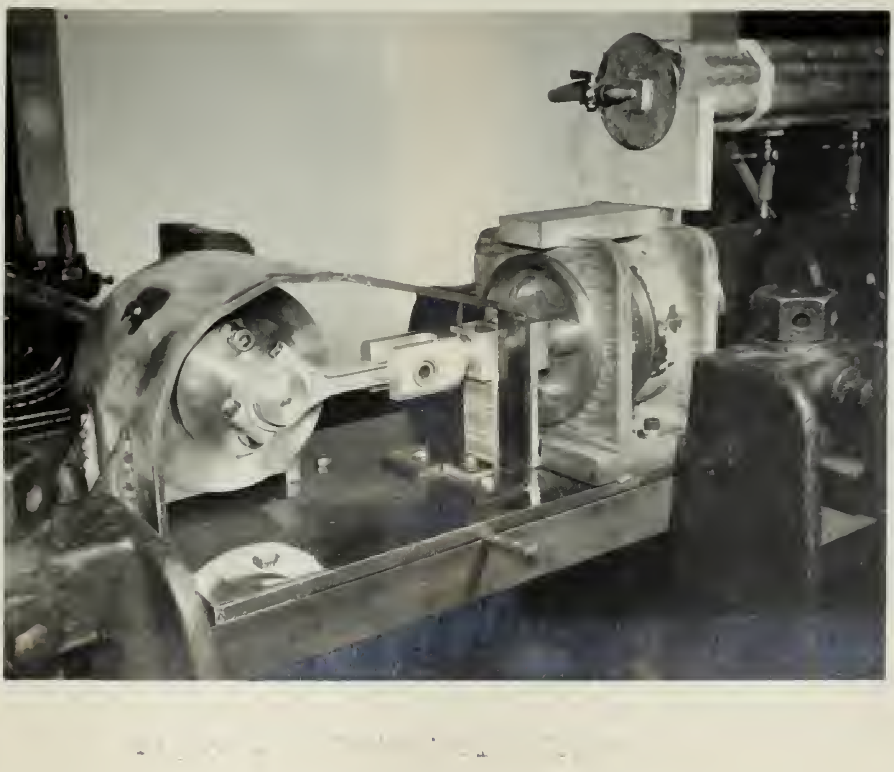

Figure 2 [illegible]

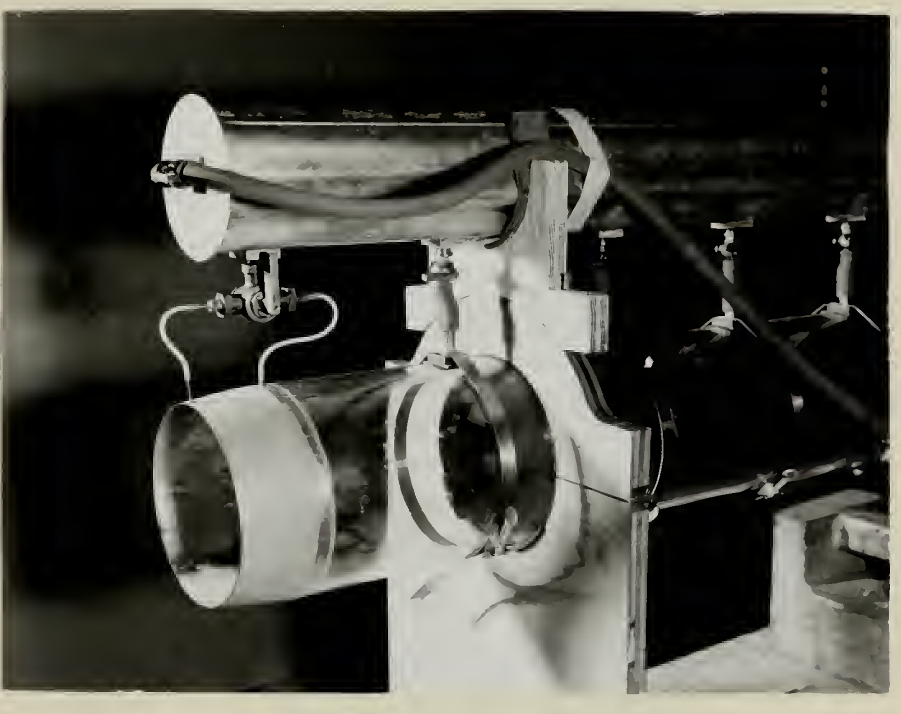

Figure 3 – Resonator Open End Modification with "Wall Static" Instrumentation.

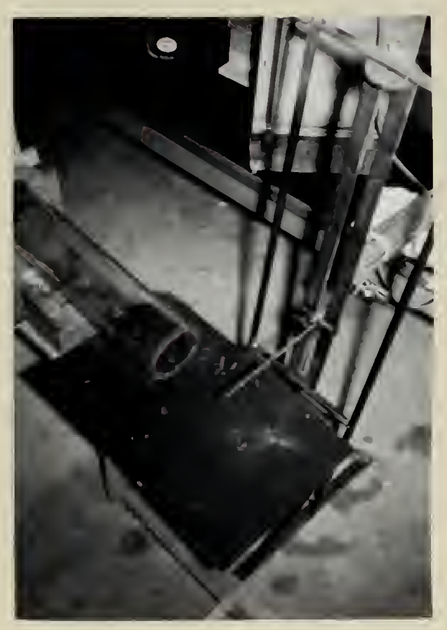

Figure 4 – External Segment Arrangement

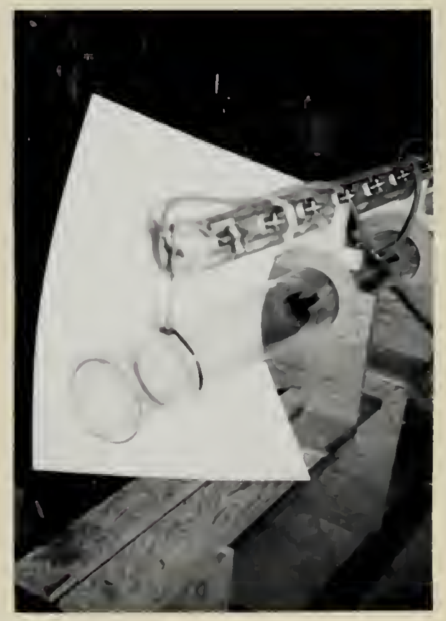

Figure 5 – Internal Segments Arrangement

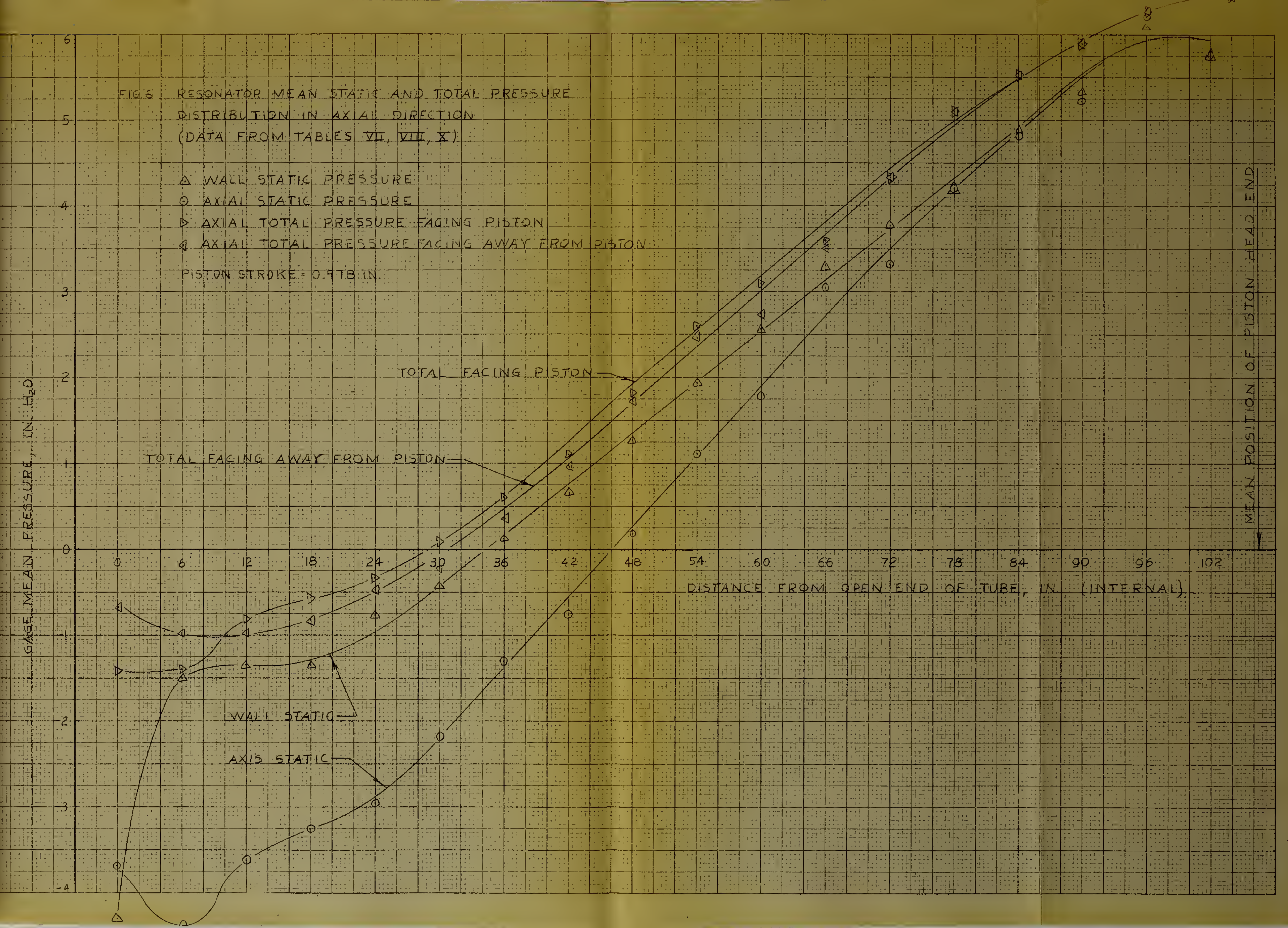

FIG. 6 RESONATOR MEAN STATIC AND TOTAL PRESSURE DISTRIBUTION IN AXIAL DIRECTION (DATA FROM TABLES VII, VIII, X)

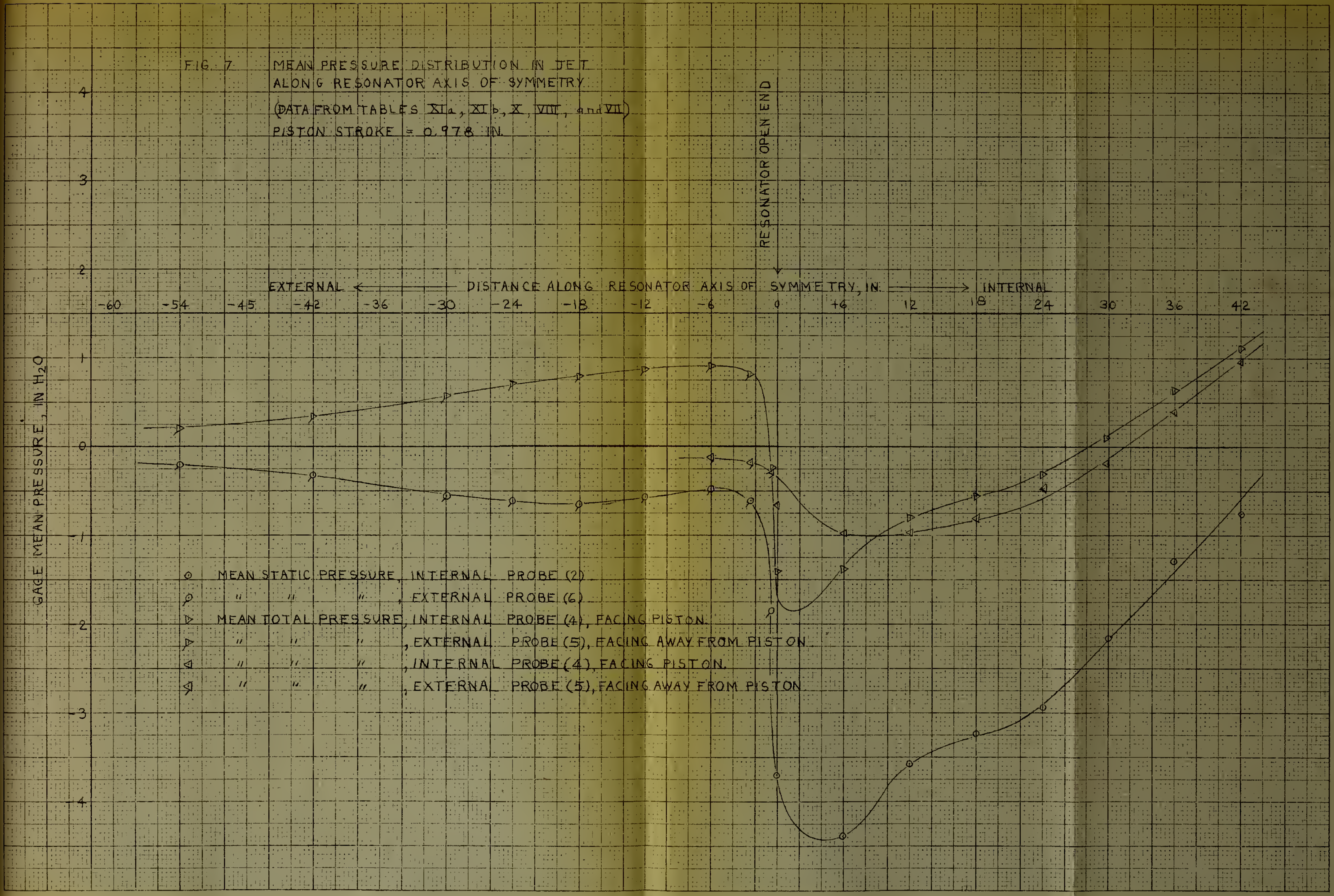

FIG. 7 MEAN PRESSURE DISTRIBUTION IN JET ALONG RESONATOR AXIS OF SYMMETRY

(DATA FROM TABLES XIa, XIb, X, VIII, and VII)

PISTON STROKE = 0.978 IN.

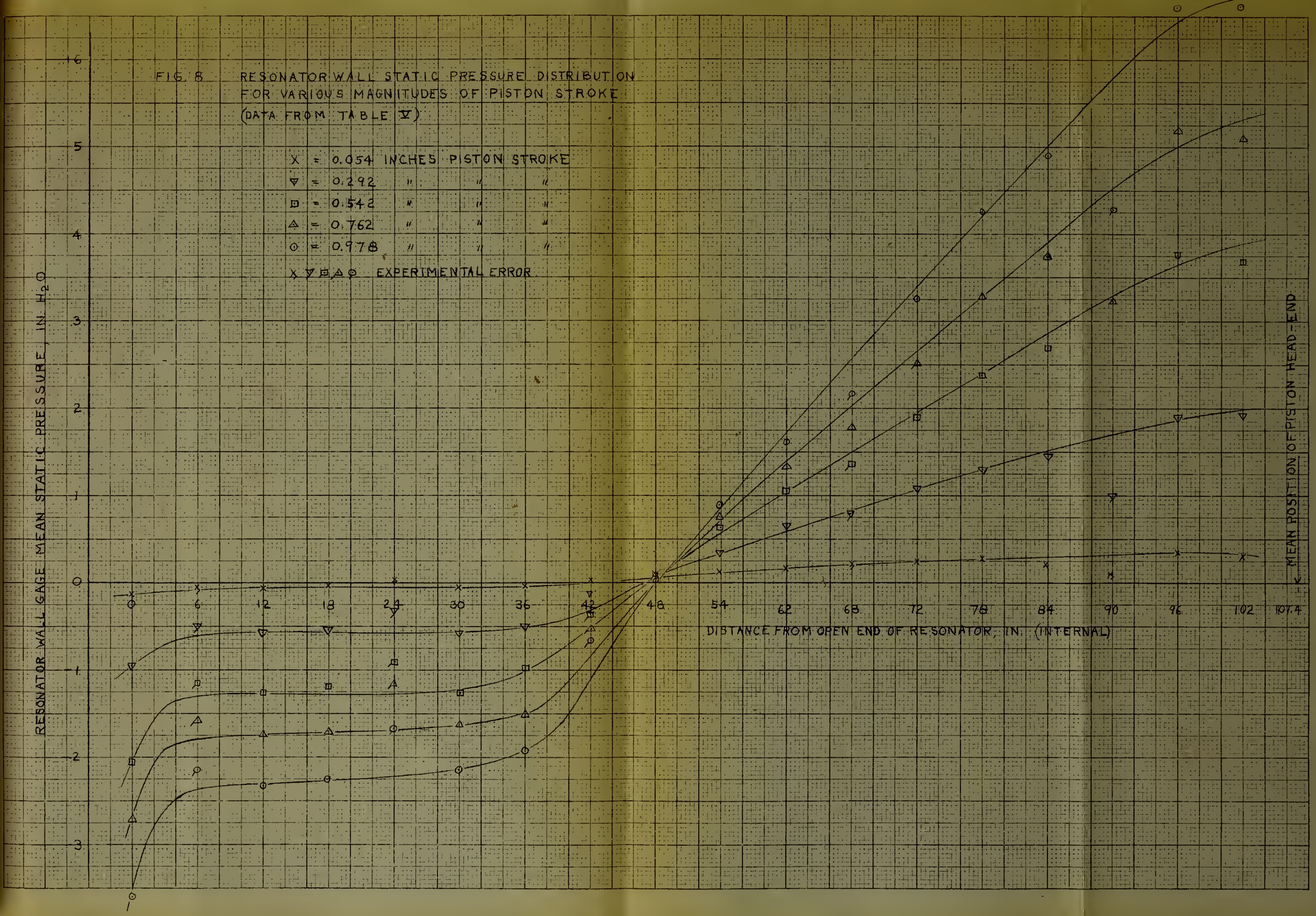

FIG. 8 RESONATOR WALL STATIC PRESSURE DISTRIBUTION FOR VARIOUS MAGNITUDES OF PISTON STROKE (DATA FROM TABLE V)

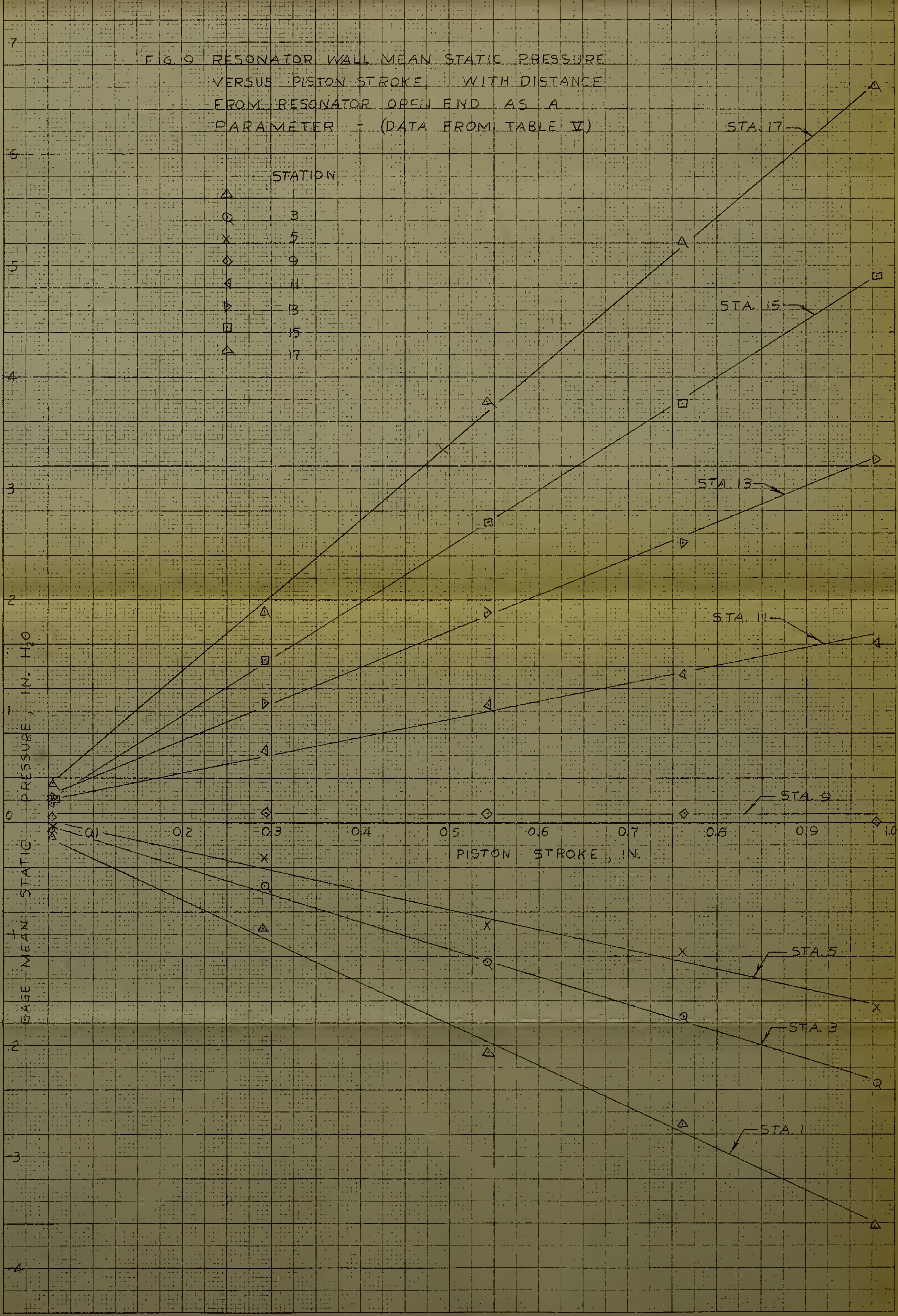

FIG. 9 RESONATOR WALL MEAN STATIC PRESSURE VERSUS PISTON STROKE, WITH DISTANCE FROM RESONATOR OPEN END AS A PARAMETER - (DATA FROM TABLE V)

FIG. 10 EFFECT OF OPEN END SHAPE ON MEAN STATIC PRESSURE AT THE RESONATOR SURFACE

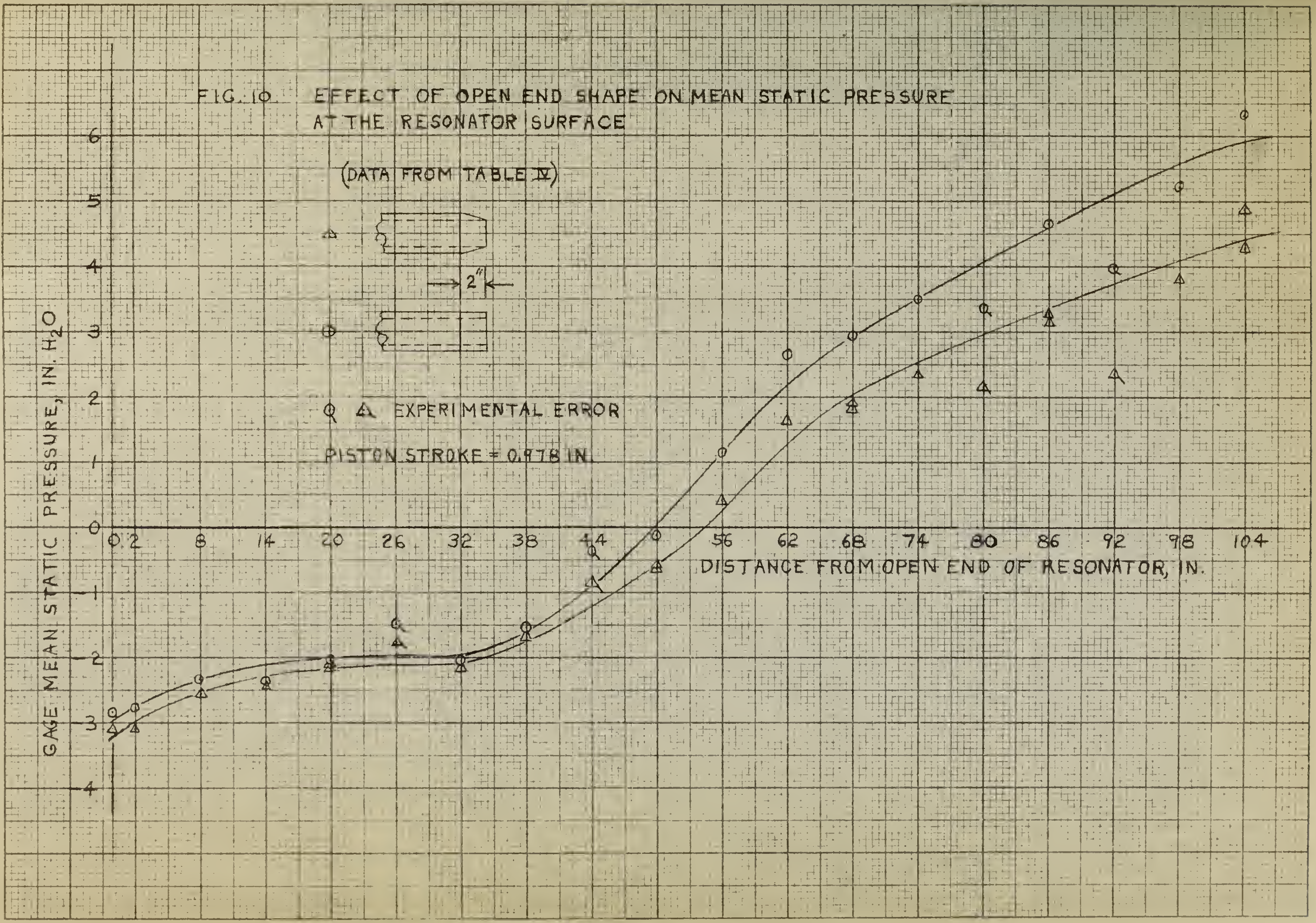

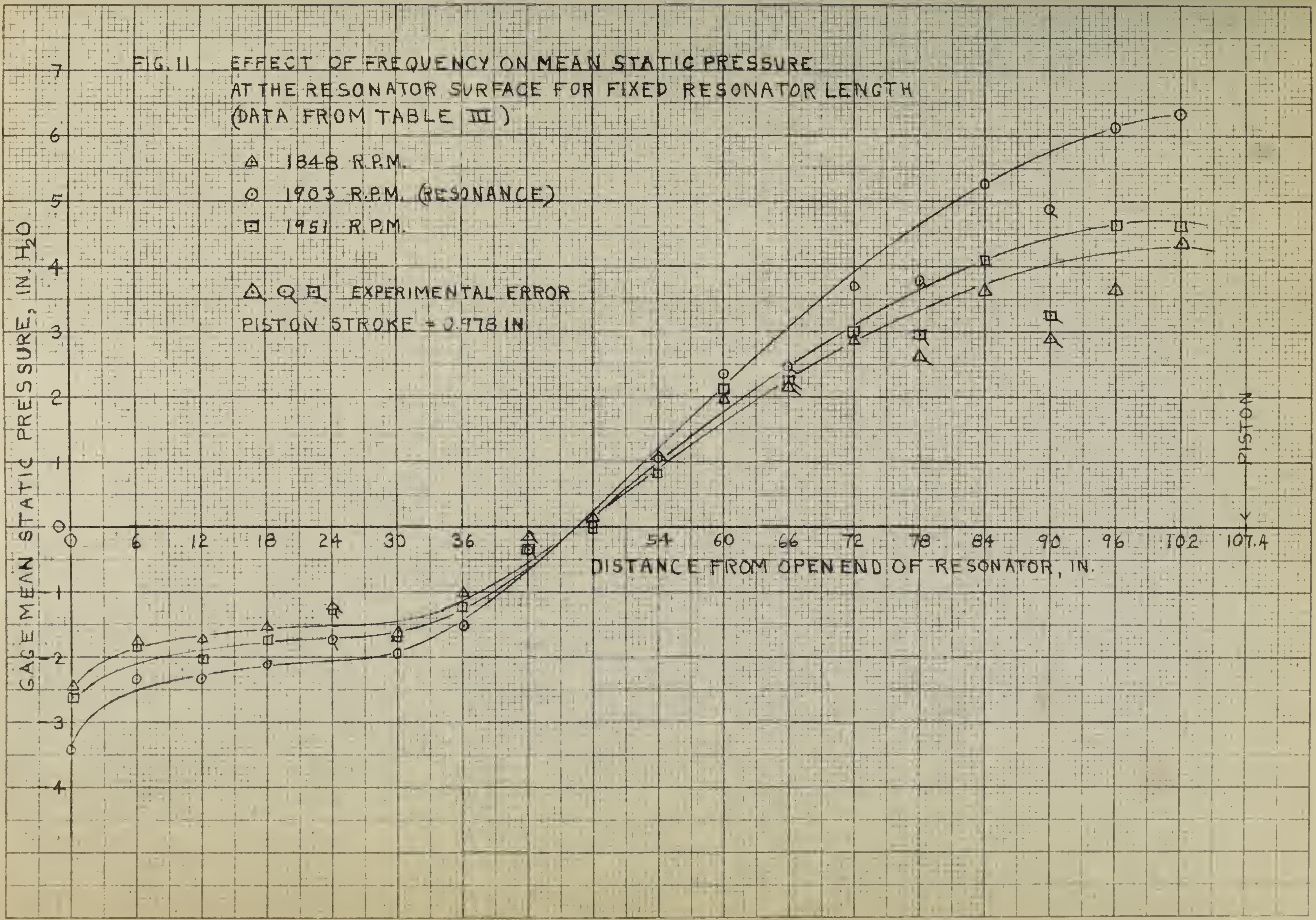

FIG. 11 EFFECT OF FREQUENCY ON MEAN STATIC PRESSURE AT THE RESONATOR SURFACE FOR FIXED RESONATOR LENGTH (DATA FROM TABLE III)

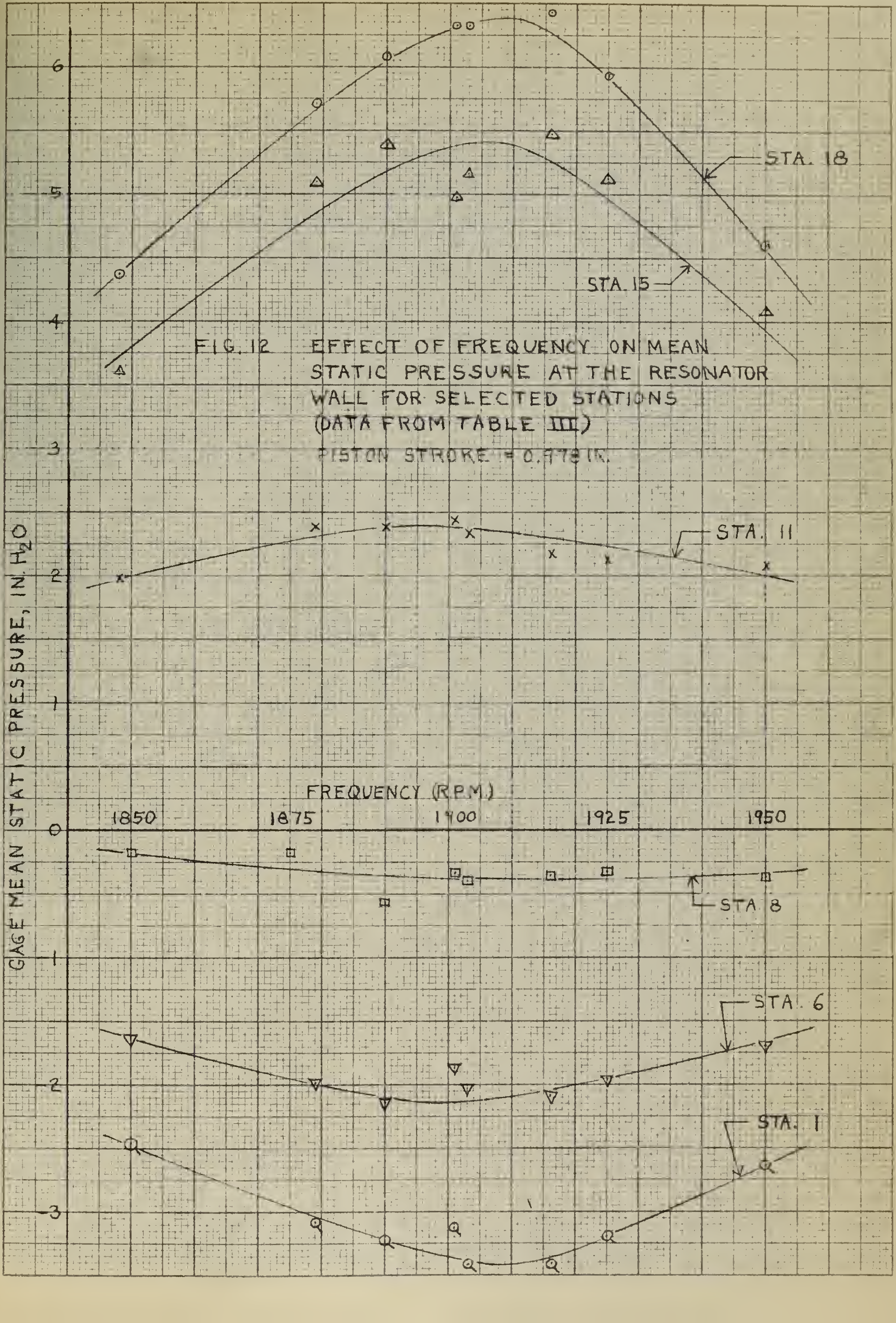

FIG. 12 EFFECT OF FREQUENCY ON MEAN STATIC PRESSURE AT THE RESONATOR WALL FOR SELECTED STATIONS

(DATA FROM TABLE III)

PISTON STROKE = 0.978 IN.

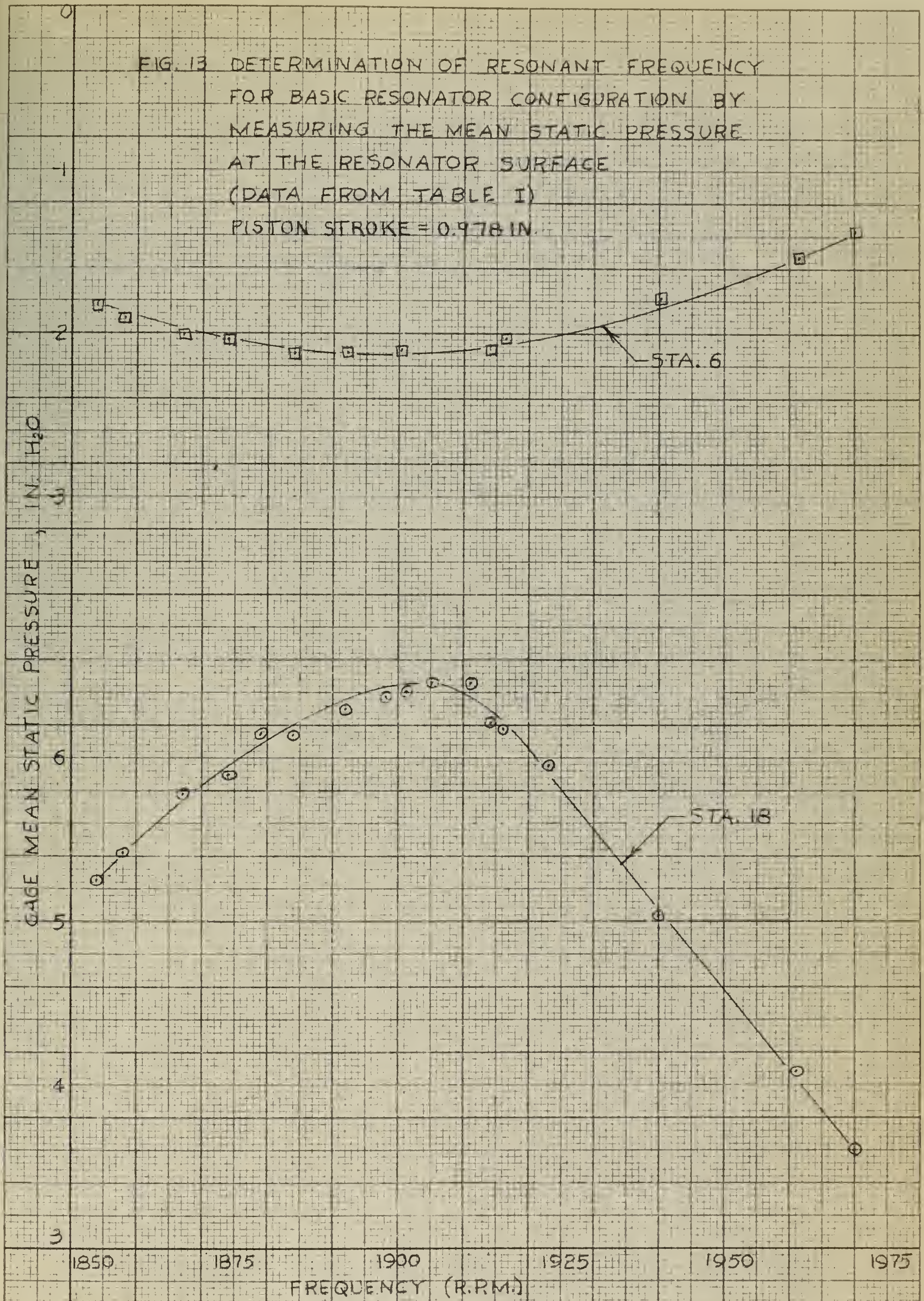

FIG. 13 DETERMINATION OF RESONANT FREQUENCY FOR BASIC RESONATOR CONFIGURATION BY MEASURING THE MEAN STATIC PRESSURE AT THE RESONATOR SURFACE (DATA FROM TABLE I)

PISTON STROKE = 0.978 IN.

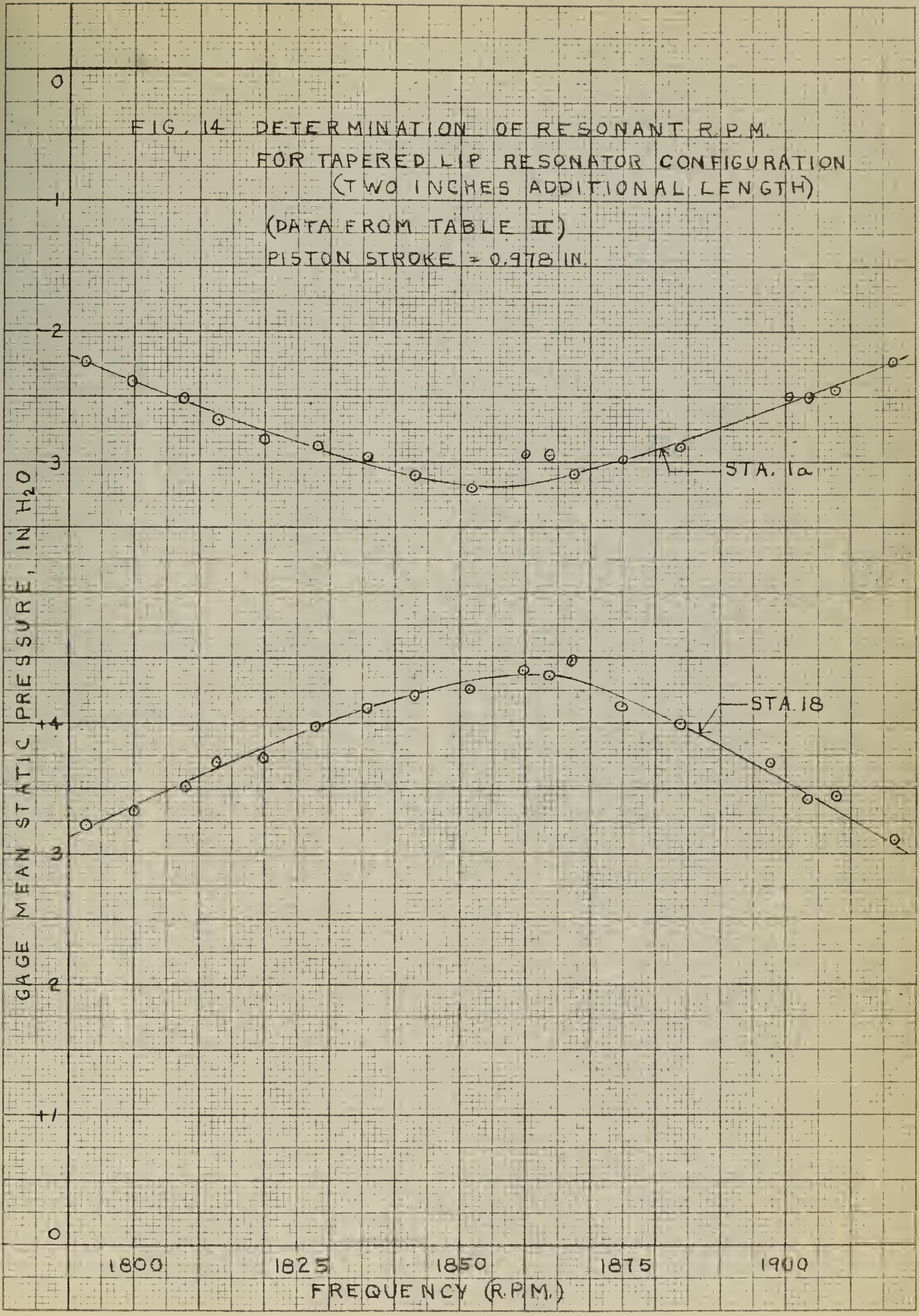

FIG. 14 DETERMINATION OF RESONANT R.P.M. FOR TAPERED LIP RESONATOR CONFIGURATION (TWO INCHES ADDITIONAL LENGTH)

(DATA FROM TABLE II)
PISTON STROKE = 0.978 IN.

FIG 15 THRUST FOR BASIC RESONATOR CONFIGURATION.
(DATA FROM TABLE VI)

L = 107.4 IN.
D = 5.5 IN.

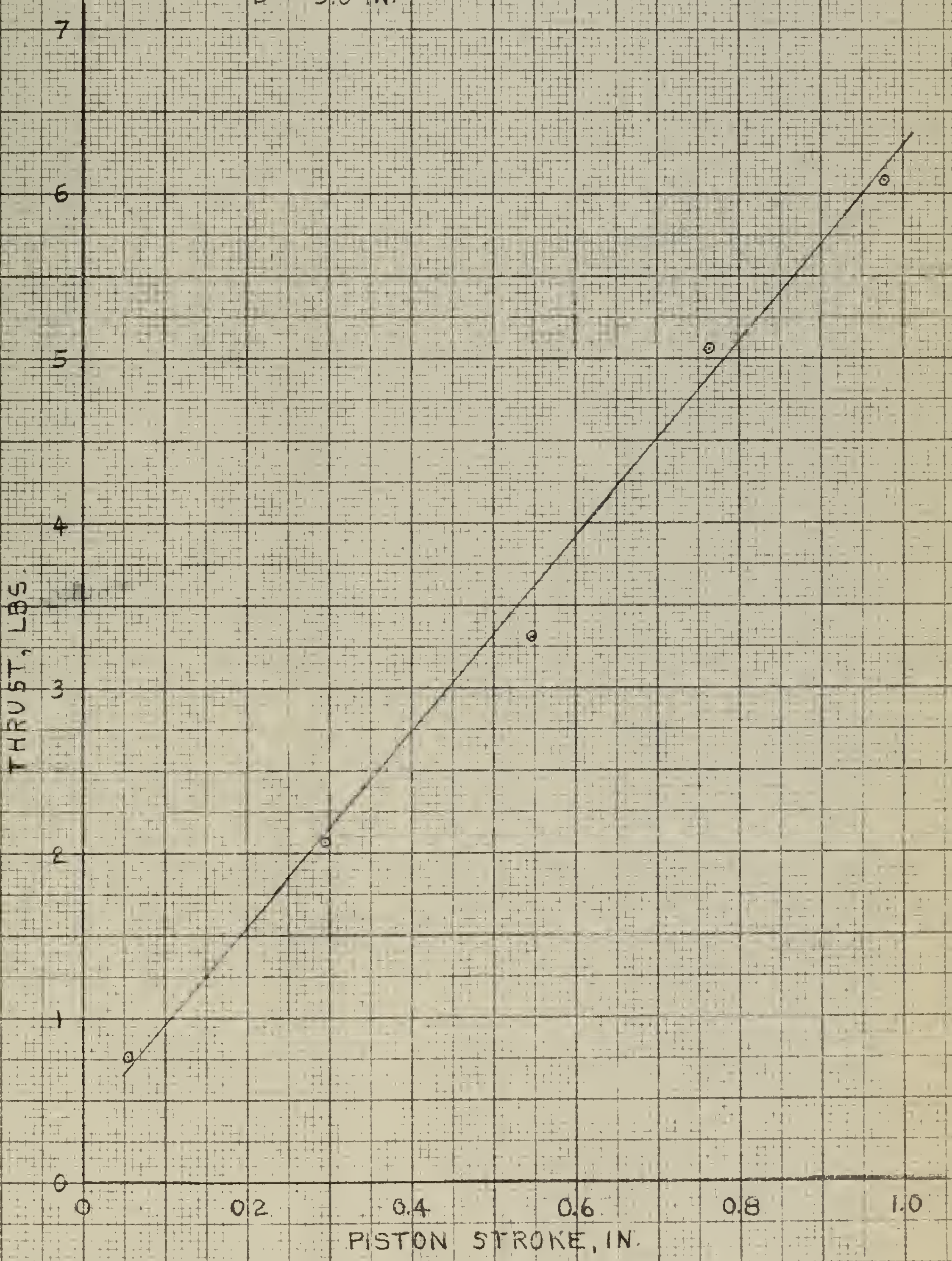

FIG. 16 INTERNAL RADIAL TRAVERSE,
MEAN STATIC PRESSURE
(DATA FROM TABLE VII)
PISTON STROKE = 0.978 IN.

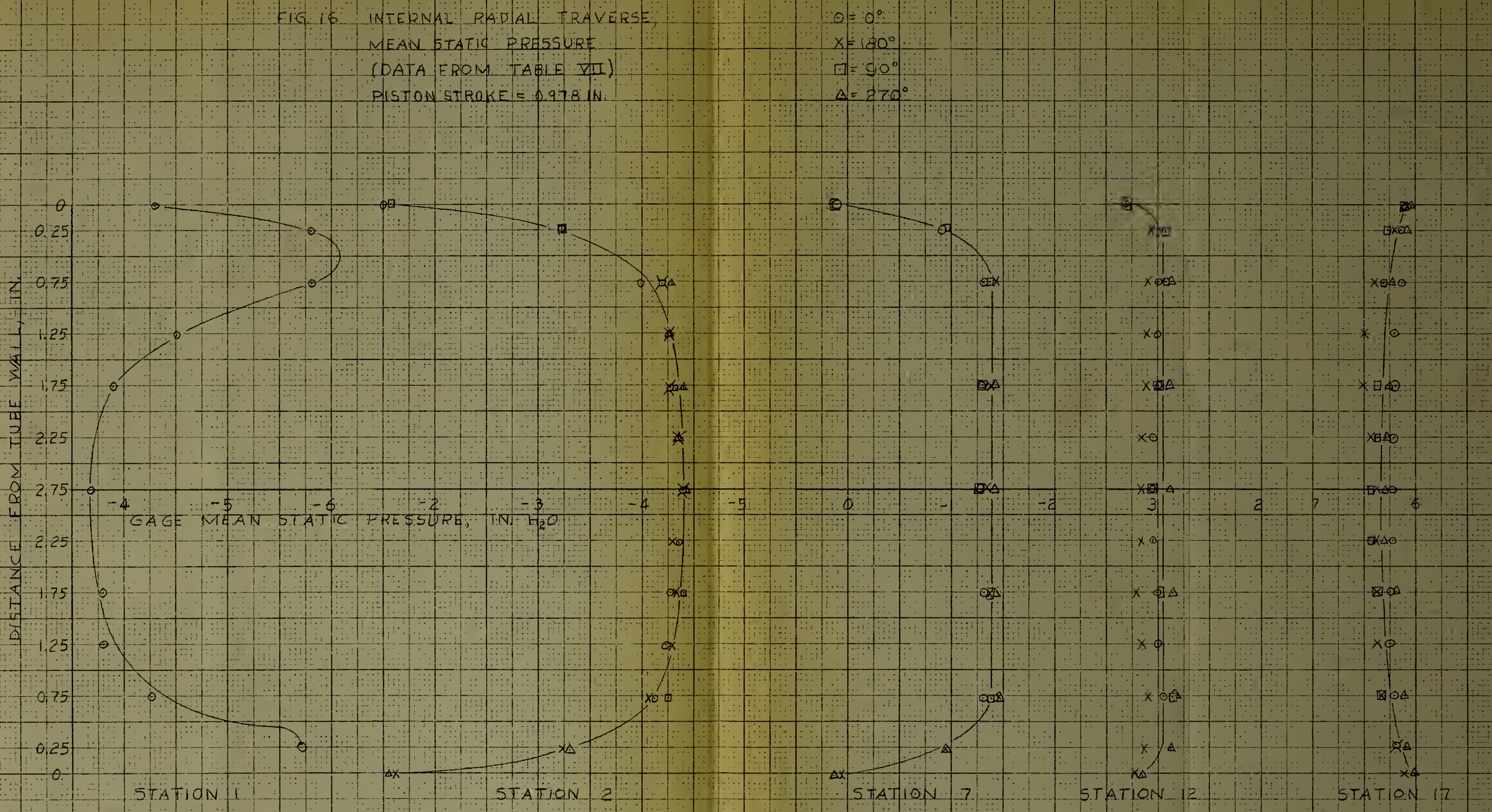

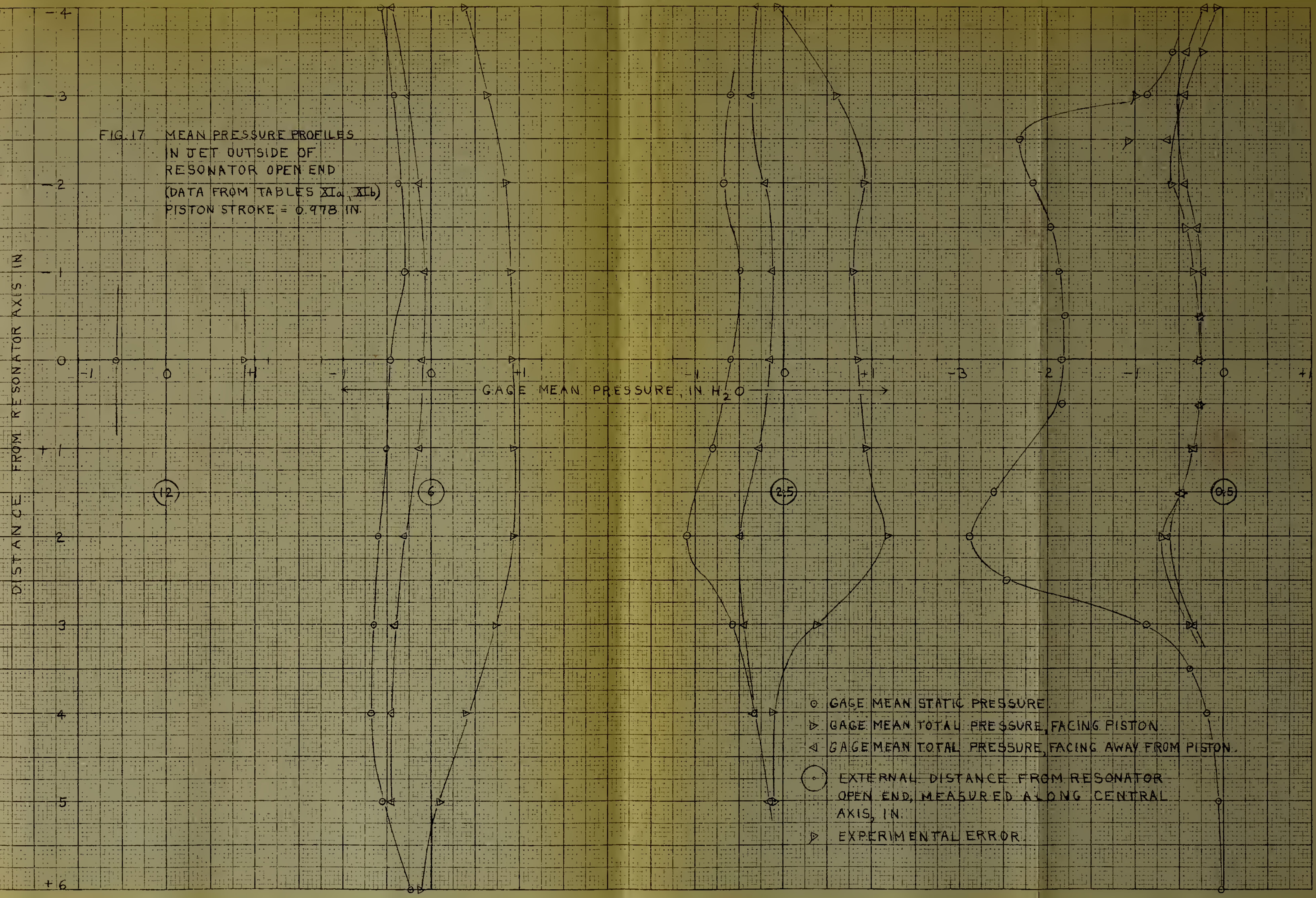

FIG. 17 MEAN PRESSURE PROFILES IN JET OUTSIDE OF RESONATOR OPEN END

(DATA FROM TABLES XIa, XIb)

PISTON STROKE = 0.978 IN.

FIG. 18 INTERNAL RADIAL TRAVERSE
MEAN TOTAL PRESSURE
(DATA FROM TABLE IX)
PISTON STROKE = 0.978 IN.

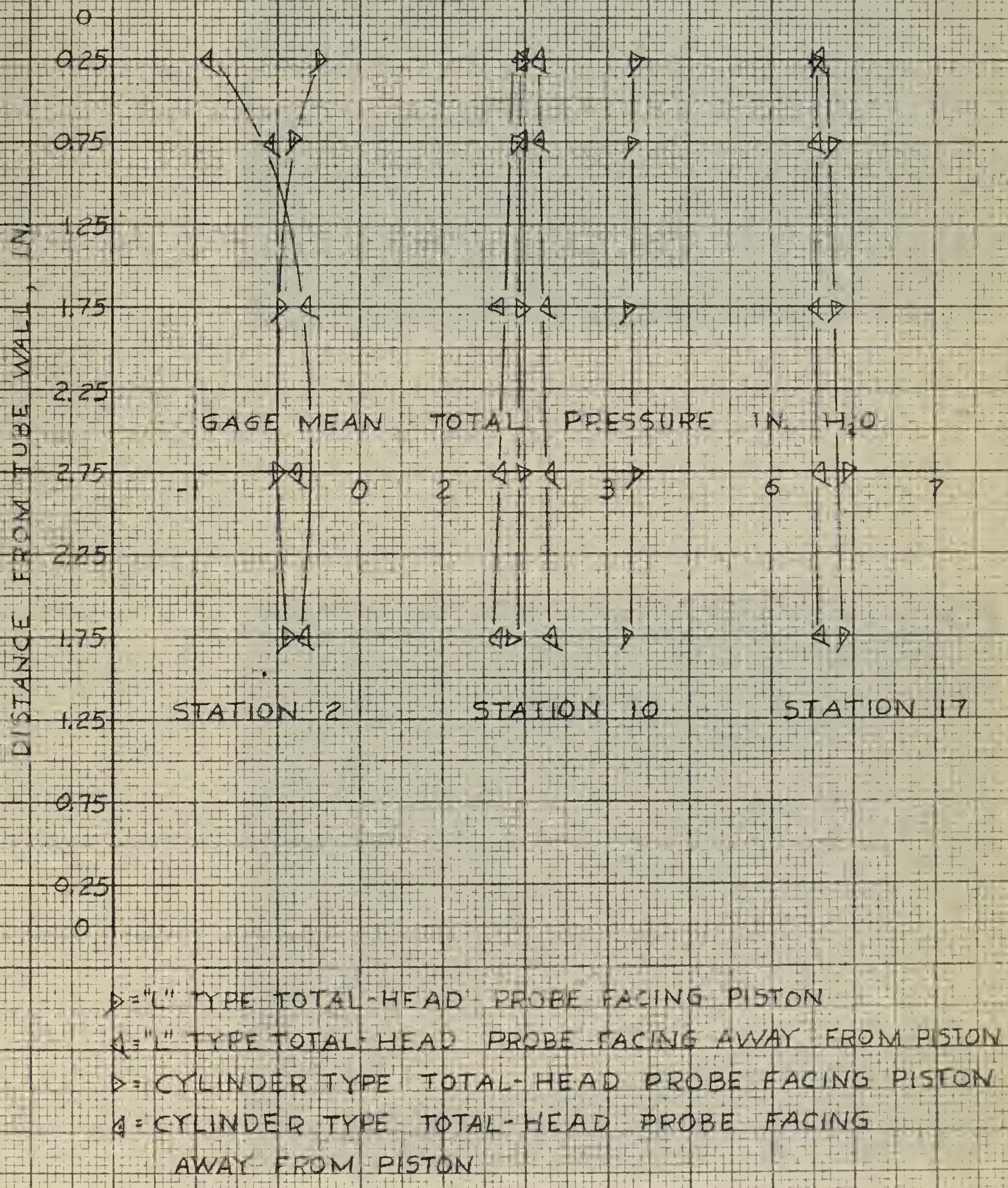

[illegible]

[illegible]

[illegible]

[illegible]

[illegible]

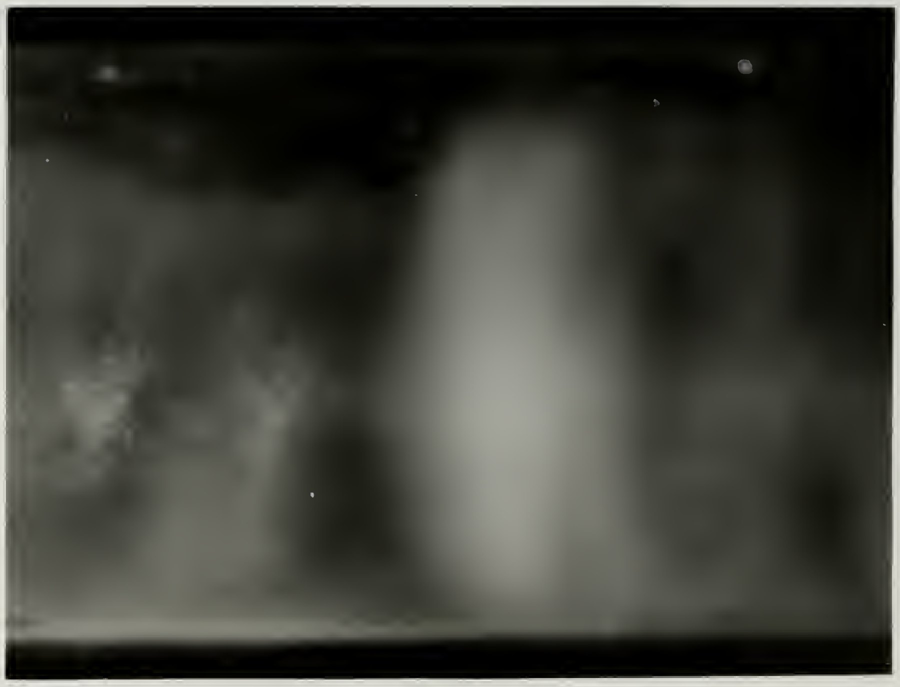

[illegible]

[illegible]

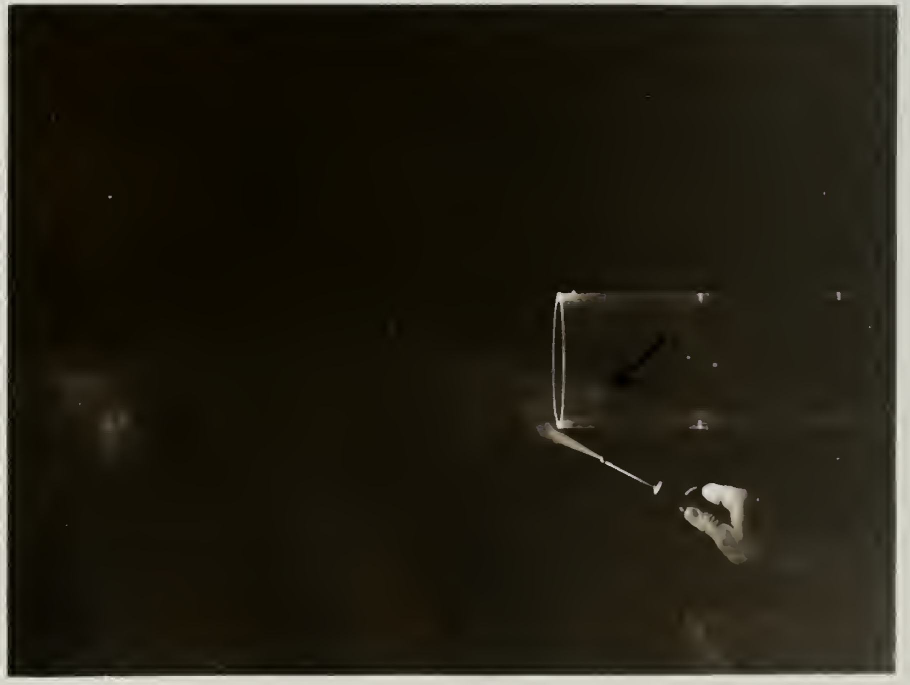

[illegible]

FIG. 27 VARIATION OF DEPTH OF PENETRATION OF RESONATOR, BY END VORTEX SYSTEM, WITH MAGNITUDE OF PISTON STROKE.
(DATA FROM TABLE XII)

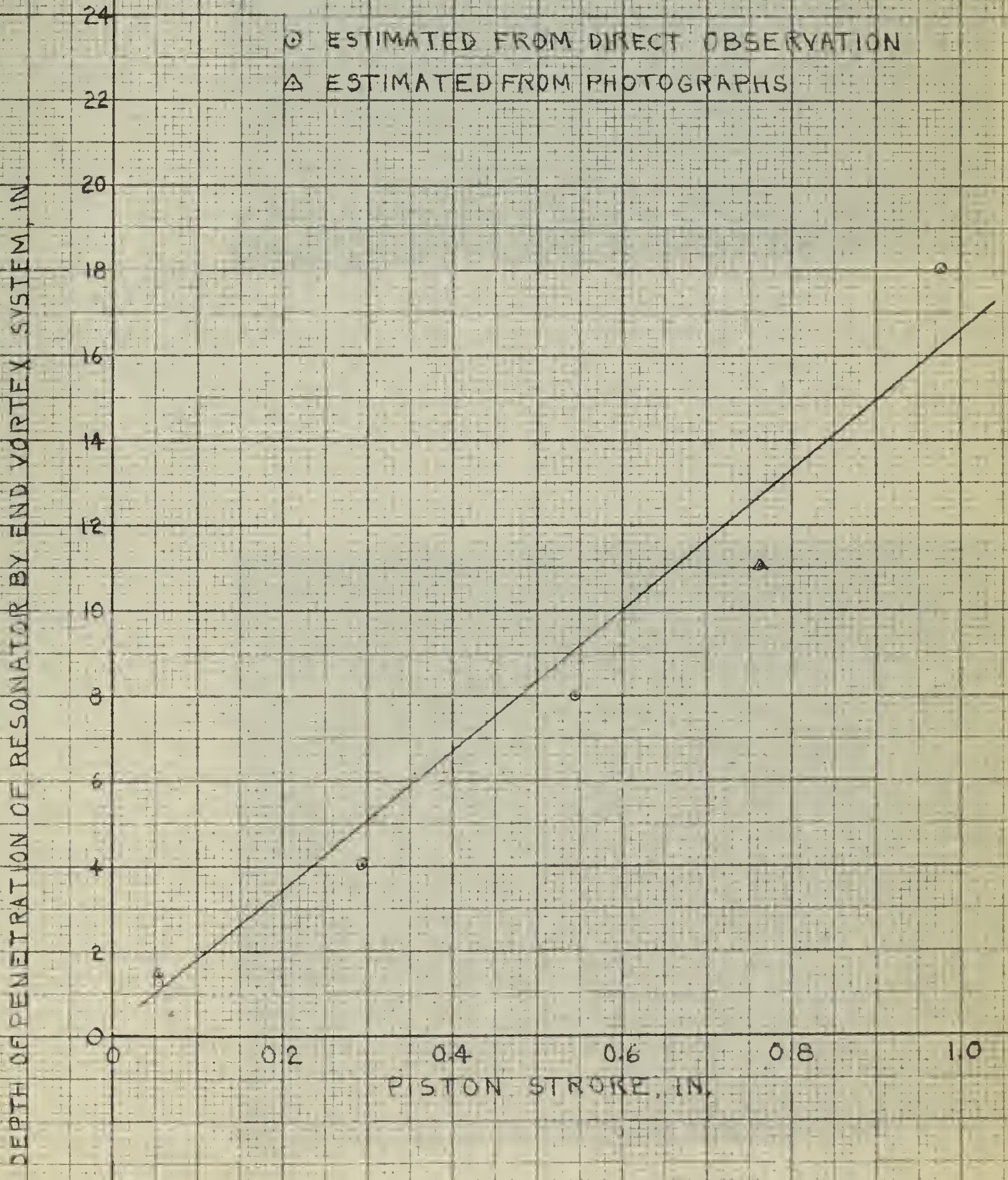

[illegible]

[illegible]

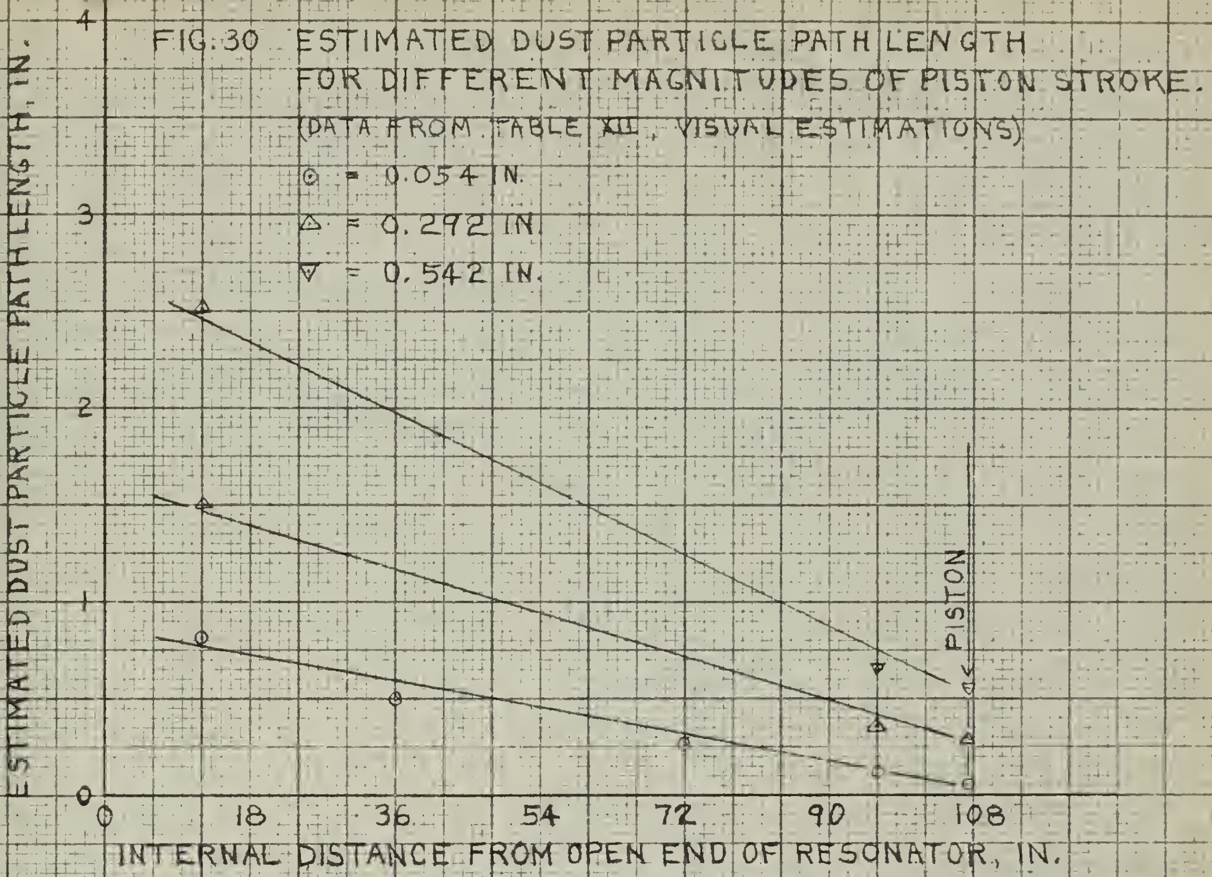

FIG. 30 ESTIMATED DUST PARTICLE PATH LENGTH FOR DIFFERENT MAGNITUDES OF PISTON STROKE.

(DATA FROM TABLE XII, VISUAL ESTIMATIONS)

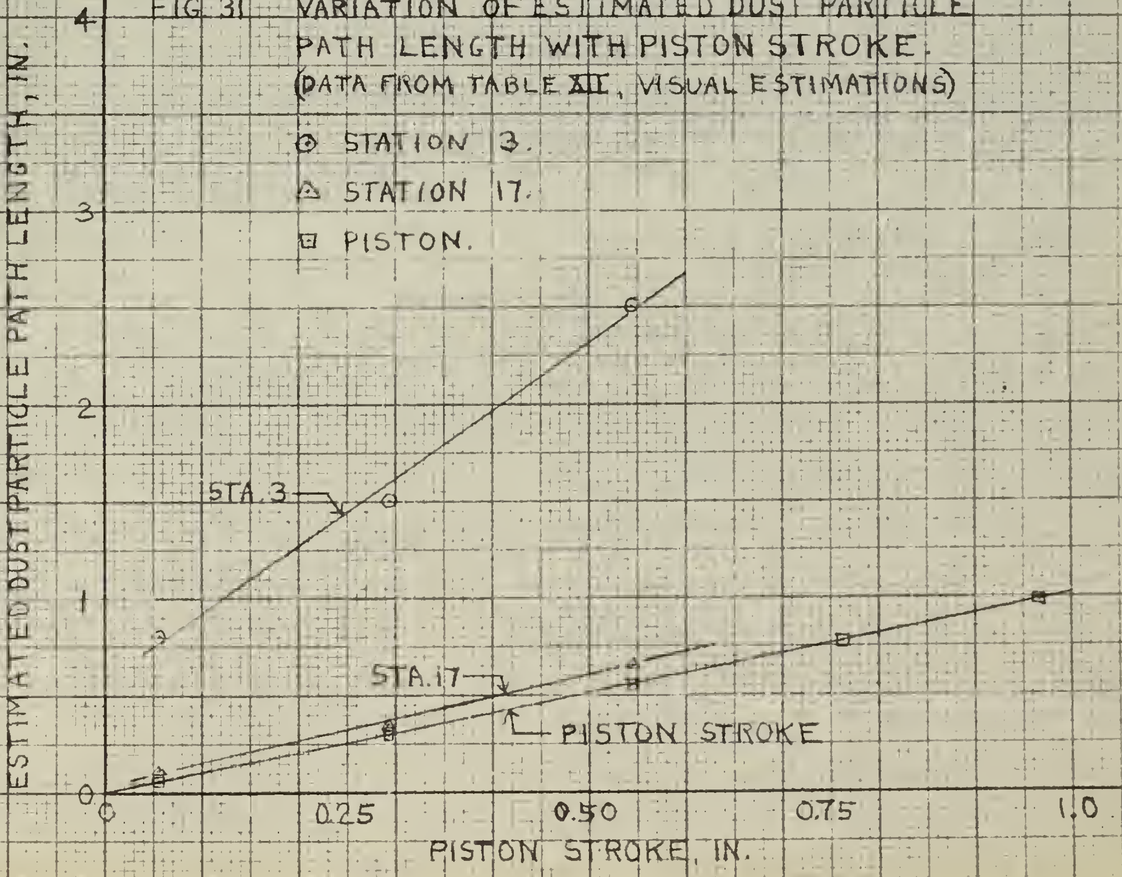

FIG. 31 VARIATION OF ESTIMATED DUST PARTICLE PATH LENGTH WITH PISTON STROKE.

(DATA FROM TABLE XII, VISUAL ESTIMATIONS)

FIG **32** IDEALIZED TIME-DISTANCE DIAGRAM OF WAVE PROGRESS IN A RESONATOR CLOSED AT ONE END BY A PULSATOR AND OPEN AT THE OTHER END

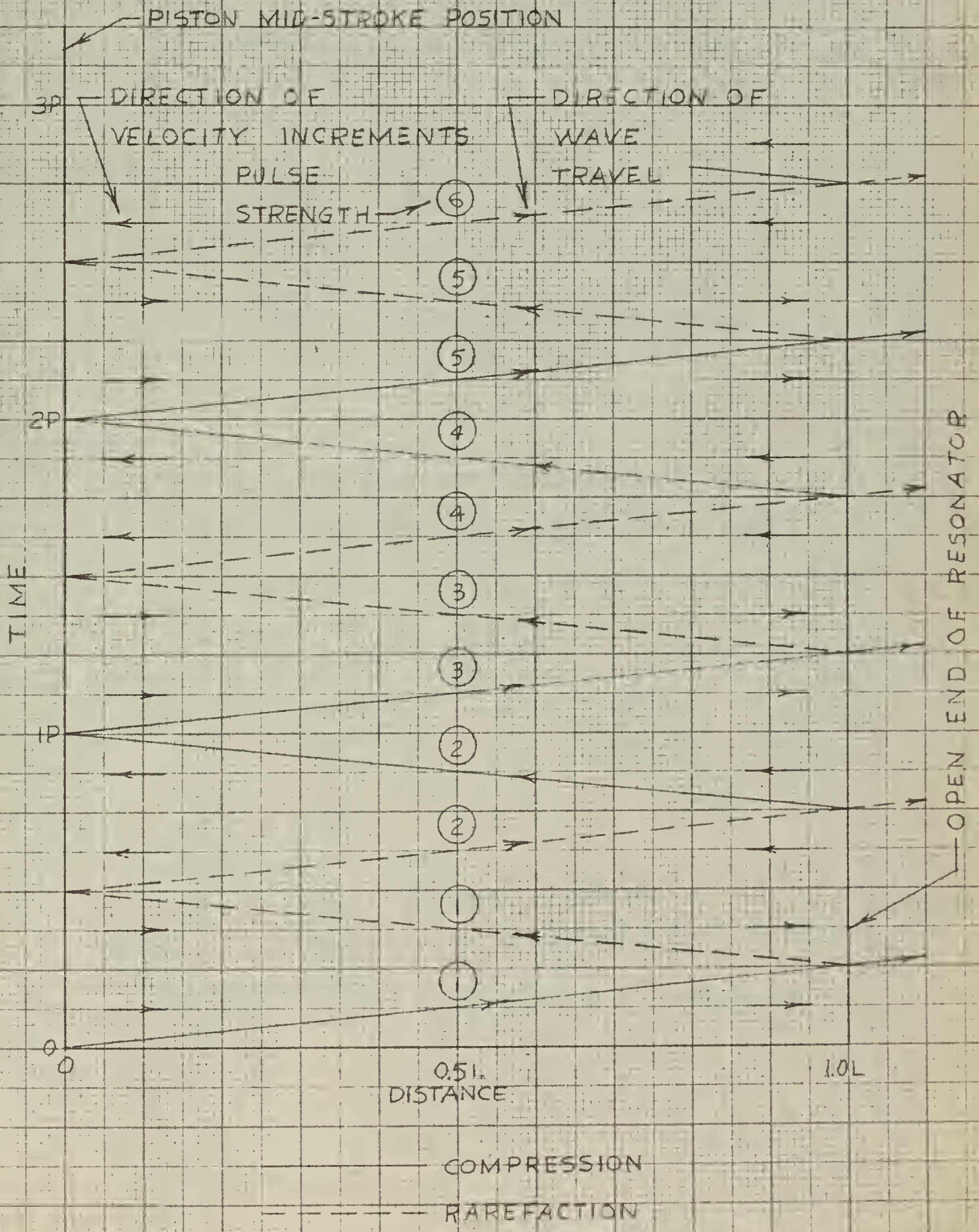
PISTON MID-STROKE POSITION
3P
2P
1P
0
DIRECTION OF VELOCITY INCREMENTS
PULSE STRENGTH
DIRECTION OF WAVE TRAVEL
①
②
③
④
⑤
⑥
TIME
OPEN END OF RESONATOR
0
0.5L
1.0L
DISTANCE
COMPRESSION
RAREFACTION

SAMPLE CALCULATIONS

RESONATOR FREQUENCY:

$r = 2.75$ in.; $L = 107.4$ in.; $t = 88$°F (Table I);

$$f = \frac{12 \cdot 1148}{4\left[107.4 + 0.6(2.75)\right]} = 31.63 \text{ c.p.s.} = 1898 \text{ R.P.M.}$$

VELOCITY:

$h_o = -0.67$ in. H_2O (Table X, Sta. 1)

$h_s = -3.68$ in. H_2O (Table VIII, Sta. 1)

$$V = \sqrt{\frac{2(p_o - p_s)}{\rho}} = \sqrt{\frac{2(64.2)(3.68 - 0.67)}{(12)(0.002378)}} = 116 \text{ ft./sec.}$$

THRUST:

$H_a = 29.42$ in. Hg $= 400$ in. H_2O (Table V).

$h_{s(piston)} = h_{s_p} = +6.6$ in. H_2O (Fig. 8, uncorrected)

$h_{s(open\ edge)} = h_{s_e} = -3.6$ in. H_2O (Fig. 8, uncorrected).

$$T = p_{s_p} \cdot A_p + p_{s_e} \cdot A_e - p_a \pi (3)^2$$

p_{s_p} = absolute pressure on piston, lbs/in.^{2}

p_{s_e} = " " " open-end edge, lbs/in.^{2}

p_a = " " ", atmospheric assumed acting externally on unit.

A_p = piston area $= \pi(2.75)^2 = 23.80$ in^2

A_e = open-end edge area $= \pi(3)^2 - A_p = 4.48$ in^2.

$$T = \frac{62.4}{12 \cdot 144}\left[406.6(23.8) + 396.4(4.48) - 400(28.28)\right]$$

$= 6.06$ lbs.

5/9

DATE DUE

16259

Thesis
J28

Janes

Investigation of the air-flow in an acoustic jet a resonance.

Thesis 16259
J28 Janes
Investigation of the air-flow in an acoustic jet a resonance.

thesJ28
Investigation of the air-flow in an acou

3 2768 002 10015 8
DUDLEY KNOX LIBRARY